

Measurement of pseudorapidity distributions of charged particles in proton–proton collisions at $\sqrt{s} = 8$ TeV by the CMS and TOTEM experiments

The CMS and TOTEM Collaborations*

CERN, 1211 Geneva 23, Switzerland

Received: 4 May 2014 / Accepted: 31 August 2014 / Published online: 29 October 2014

© CERN for the benefit of the CMS and TOTEM collaborations 2014. This article is published with open access at Springerlink.com

Abstract Pseudorapidity (η) distributions of charged particles produced in proton–proton collisions at a centre-of-mass energy of 8 TeV are measured in the ranges $|\eta| < 2.2$ and $5.3 < |\eta| < 6.4$ covered by the CMS and TOTEM detectors, respectively. The data correspond to an integrated luminosity of $\mathcal{L} = 45 \mu\text{b}^{-1}$. Measurements are presented for three event categories. The most inclusive category is sensitive to 91–96 % of the total inelastic proton–proton cross section. The other two categories are disjoint subsets of the inclusive sample that are either enhanced or depleted in single diffractive dissociation events. The data are compared to models used to describe high-energy hadronic interactions. None of the models considered provide a consistent description of the measured distributions.

1 Introduction

Measurements of the yields and kinematic distributions of particles produced in proton–proton (pp) collisions at the Large Hadron Collider (LHC) can provide a better understanding of the mechanisms of hadron production in high-energy hadronic interactions. Two types of processes contribute to the production of most of the final-state particles at LHC energies. Semi-hard (multi)parton scattering, with exchanged momenta of a few GeV, is the dominant contribution. Diffractive scattering in more peripheral pp interactions, where one or both protons survive the interaction and/or are excited into a low-mass state, accounts for 15–40 % [1, 2] of the pp inelastic cross section. As the particle multiplicity produced in these processes is modelled phenomenologically in the existing Monte Carlo (MC) event generators of hadronic interactions, experimental results provide an important input for tuning of the models.

The results presented here focus on the charged-particle multiplicity density ($dN_{\text{ch}}/d\eta$, also referred to as the pseudorapidity distribution) corrected down to zero transverse momentum (p_{T}), in the pseudorapidity ranges $|\eta| < 2.2$ and $5.3 < |\eta| < 6.4$, where η is defined as $-\ln[\tan(\theta/2)]$, with θ being the polar angle of the particle trajectory with respect to the anticlockwise-beam direction. Inclusive measurements of the η and p_{T} distributions of charged particles have previously been performed in pp and p \bar{p} collisions for different centre-of-mass energies and phase space regions [3–14].

In this paper, the data samples were collected with a minimum bias trigger generated by at least one arm of the TOTEM T2 telescopes, which also triggered the readout of the Compact Muon Solenoid (CMS). Three event samples with different final-state topologies are selected offline: a sample of inclusive inelastic pp events, a sample dominated by non-single diffractive dissociation (NSD) events and a sample enriched in single diffractive dissociation (SD) events. The measured data are compared to the predictions of MC event generators that model pp collider data and high-energy cosmic ray hadronic interactions.

2 Experimental setup

The CMS and TOTEM experiments use a right-handed coordinate system, with the origin at the nominal interaction point (IP), the x -axis pointing to the centre of the LHC ring, the y -axis pointing upwards and the z -axis pointing along the anticlockwise-beam direction. The azimuthal angle, ϕ , is measured in the (x, y) plane, where $\phi = 0$ is the $+x$ and $\phi = \pi/2$ is the $+y$ direction.

A complete description of the CMS detector can be found in Ref. [15]. The central feature of the CMS apparatus is a superconducting solenoid of 6 m internal diameter, providing a uniform magnetic field of 3.8 T parallel to the beam axis. Inside the magnetic field are the pixel tracker, the silicon-strip tracker, the lead tungstate electromagnetic calorime-

* e-mails: cms-publication-committee-chair@cern.ch;
Totem-EB@cern.ch

ter and the brass/scintillator hadron calorimeter. Muons are measured in gas-ionisation detectors embedded in the steel return yoke outside the solenoid. In addition to the barrel and endcap detectors, which extend up to $|\eta| = 3.0$, the steel/quartz-fibre hadron forward calorimeters (HF) cover the region $2.9 < |\eta| < 5.2$. The tracking detector consists of 1440 silicon pixel and 15 148 silicon strip detector modules. The barrel is composed of 3 pixel and 10 strip layers around the interaction point at radii from 4.4 to 110 cm. The forward and backward endcaps each consist of 2 pixel disks and 12 strip disks in up to 9 rings. Three of the strip rings and four of the barrel strip layers contain an additional plane, with a stereo angle of 100 mrad, to provide a measurement of the r -coordinate and z -coordinate, respectively. The tracker is designed to provide a longitudinal and transverse impact parameter resolution of about 100 μm and a p_T resolution of about 0.7 % for 1 GeV/c charged particles at $\eta = 0$ [16].

The TOTEM experiment [17, 18] is composed of three subdetectors: the Roman pots and the T1 and T2 telescopes. Minimum bias events are triggered by the two T2 telescopes, which are placed symmetrically on each side of the IP at about $|z| = 14$ m. They detect charged particles produced in the polar angular range of $\approx 3\text{--}10$ mrad ($5.3 < |\eta| < 6.5$), with full azimuthal acceptance. Each telescope consists of two half-arms, with each half-arm composed of 10 semicircular planes of triple-GEM (gas electron multiplier) chambers, arranged within a 40 cm space along the z -axis. Each chamber provides two-dimensional information on the track position covering 192° in azimuthal angle with a small vertical overlap region between chambers of two neighbouring half-arms. Every chamber has a double-layered read-out board containing two columns of 256 concentric strips (400 μm pitch, 80 μm width) to measure the radial coordinate and a matrix of 1560 pads, each covering $\Delta\eta \times \Delta\phi \approx 0.06 \times 0.018$ rad, to measure the azimuthal coordinate, and for triggering. The radial and azimuthal coordinate resolutions are about 110 μm and 1° , respectively [19]. Local angles of single tracks are reconstructed with an average resolution of 0.5 mrad, and the track pseudorapidity resolution for charged particles is better than 0.05 [20], once the track is identified as coming from the vertex.

The detailed MC simulations of the CMS and TOTEM detectors are based on GEANT4 [21]. Simulated events are processed and reconstructed in the same manner as collision data.

3 Monte Carlo models

Various MC event generators for hadronic collisions are used for data corrections and for comparison with the final, fully corrected results. The PYTHIA6 (version 6.426) [22] generator is used with tune Z2* and PYTHIA8 (version 8.153) [23] with

tune 4C [24]. These programs provide different descriptions of the diffractive component and they both use a model [25] in which multiple partonic interactions are interleaved with parton showering. The Z2* tune [26] uses the CTEQ6L1 [27] parton distribution function (PDF) set. Tune 4C of PYTHIA8 is based on early LHC data [24]. Parton showers in PYTHIA8 are modelled according to the Dokshitzer–Gribov–Lipatov–Altarelli–Parisi (DGLAP) [28–30] prescription and hadronisation is based on the Lund string fragmentation model [31]. Diffractive cross sections are described by the Schuler–Sjöstrand model [32]. In PYTHIA6, particle production from a low-mass state, X , with $M_X < 1 \text{ GeV}/c^2$ is treated as an isotropic two-body decay, while for high-mass states it is based on the string model. In PYTHIA8, the same model is used to generate the cross section and the diffractive mass, but particle production is modelled differently. For low-mass states, the string model is used, but for higher masses ($M_X > 10 \text{ GeV}/c^2$) a perturbative description of pomeron–proton scattering is introduced, based on diffractive PDFs [33–35], which represent probability distributions for partons in the proton under the constraint that the proton emerges intact from the collision. The non-perturbative string model introduces a mass dependence on the relative probability for a pomeron to couple to a quark or a gluon [36]. The perturbative treatment of pomeron–proton scattering results in harder p_T spectra and higher multiplicity for diffractive events generated with PYTHIA8 than for those obtained with PYTHIA6.

The HERWIG++ (version 2.5.0) [37] MC event generator, with a recent tune to LHC data (UE-EE-3 with CTEQ6L1 PDFs [27, 38]), is also used for comparison with the data. This generator is based on matrix element calculations similar to those used in PYTHIA. However, HERWIG++ features DGLAP-based parton showers ordered in angle and uses cluster fragmentation for the hadronisation [39]. The description of hard diffractive processes also makes use of diffractive PDFs; however, soft diffraction is not implemented.

The data are also compared to predictions from two MC event generators used in cosmic ray physics [40]: EPOS [41] with the LHC tune (based on EPOS 1.99) [42] and QGSJETII-04 [43]. Both models include contributions from soft- and hard-parton dynamics. The soft component is described in terms of the exchange of virtual quasi-particle states, as in Gribov’s Reggeon field theory [44], with multi-pomeron exchanges accounting for underlying-event effects. At higher energies, the interaction is described in terms of the same degrees of freedom, but generalised to include hard processes via hard-pomeron scattering diagrams, which are equivalent to a leading-order perturbative Quantum Chromodynamics (QCD) approach with DGLAP evolution. These models are retuned to LHC data [45], including cross section measurements by TOTEM, and charged-particle multiplicity measurements in the central region, by ALICE and CMS, at $\sqrt{s} = 7 \text{ TeV}$.

4 Datasets

The data were collected in July 2012 during a dedicated run with low probability ($\sim 4\%$) of overlapping pp interactions in the same bunch crossing (pileup) and a non-standard $\beta^* = 90$ m optics configuration, where β^* is the amplitude function of the beam at the interaction point. These data correspond to an integrated luminosity of $\mathcal{L} = 45 \mu\text{b}^{-1}$. A minimum bias trigger was provided by the TOTEM T2 telescopes and contributed to the CMS global trigger decision, which initiated simultaneous readout of both the CMS and the TOTEM detectors. The CMS orbit-counter reset signal delivered to the TOTEM electronics at the start of the run ensures the time synchronisation of the two experiments. Events are combined offline by requiring that both the CMS and the TOTEM reconstructed events have the same LHC orbit and bunch numbers. The minimum bias trigger required at least one track candidate (trigger track) in the T2 detector, in either z -direction [46]. With this selection the visible cross section seen by T2 has been estimated to be 91–96 % of the total pp inelastic cross section at $\sqrt{s} = 8$ TeV [47]. Zero bias data, obtained by triggering on random bunch crossings, are used to measure the trigger efficiency and to cross-check the pileup probability estimate.

MC samples were used to determine the event selection efficiency and the tracking performance. The efficiency corrections and related uncertainties for the CMS tracker are based on the PYTHIA6, PYTHIA8, and EPOS samples. The MC-based corrections for the TOTEM T2 detector and the corresponding uncertainties were determined by using PYTHIA8 and EPOS, which were found to bracket the measured $dN_{\text{ch}}/d\eta$ distributions in the forward region.

5 Event selection and track reconstruction

The T2 track reconstruction is based on a Kalman filter-like algorithm, simplified thanks to the small amount of material in the GEM planes and the weak magnetic field in the T2 region [20]. In these conditions, the particle trajectory can be successfully reconstructed with a straight-line fit. Single tracks are reconstructed with almost 100 % efficiency for $p_T > 20$ MeV/c, but because of multiple scattering and the magnetic field, tracks can be identified as coming from the IP with an efficiency that increases as a function of p_T and is greater than 80 % for $p_T > 40$ MeV/c [18]. The pseudorapidity of a track in T2 is defined as the average pseudorapidity of all T2 track hits, calculated from the angle between the z -axis and the line joining the hit and the nominal IP. This definition is adopted on the basis of MC simulation studies and gives an optimal estimation of the pseudorapidity of the selected primary (i.e. produced at the IP) particle. Because of the small scattering angle of the particles reconstructed

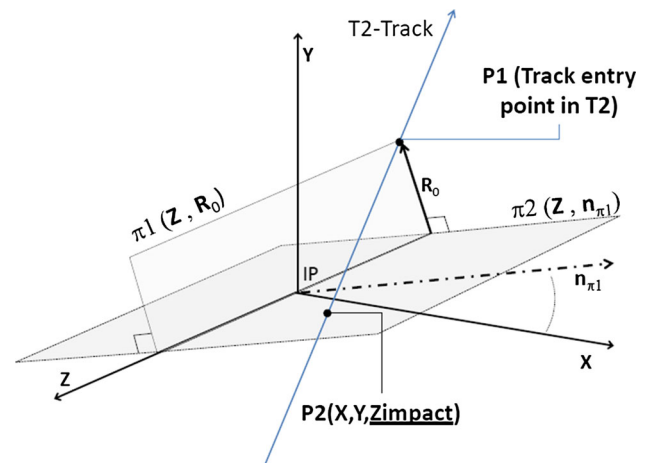


Fig. 1 Definition of the z_{impact} parameter

in T2, the position of the vertex does not affect significantly the reconstruction of the track pseudorapidity. Due to the limited number of primary particles in T2 per event, no vertex reconstruction based on T2 information is used for the analysis. The pseudorapidity region $5.4 < |\eta| < 5.6$ is not included in the analysis because of the large effect that the beam pipe cone at $|\eta| \approx 5.5$ has on the propagation of the primary particles.

About 80 % of the reconstructed tracks in T2 are due to non-primary particles, hereafter referred to as secondary particles, that are mainly electrons and positrons generated by photon conversions at the edge of the HF calorimeter of CMS and in the conical section of the beam pipe at $|\eta| \approx 5.5$. It is therefore important to discriminate these particles from the primary charged particles. The most effective primary/secondary-particle separation is achieved by using the z_{impact} track parameter (see Fig. 1), which is defined as the z coordinate of the intersection point between the track and the plane “ $\pi 2$ ”. This is the plane which contains the z -axis and is orthogonal to the plane “ $\pi 1$ ” defined by the z -axis and containing the track entry point in T2 [9]. This parameter is found to be stable against residual misalignment biases. Simulation studies demonstrate that the z_{impact} distribution in the primary-particle region can be described by the sum of two Gaussian distributions plus an exponential distribution. The Gaussians, hereafter referred to as a “double-Gaussian” distribution, are mainly due to primary particles, whereas the exponential distribution accounts for most secondary particles. Simulations predict a contamination of the double-Gaussian distribution by secondary particles of about 20 %, primarily given by photons converted in the material between the IP and T2, with a contribution from decay products of strange particles; the z_{impact} distribution of these particles is a Gaussian centred around $z_{\text{impact}} = 0$.

Figure 2 shows the z_{impact} distribution at the median η of the inclusive forward pseudorapidity distribution. A com-

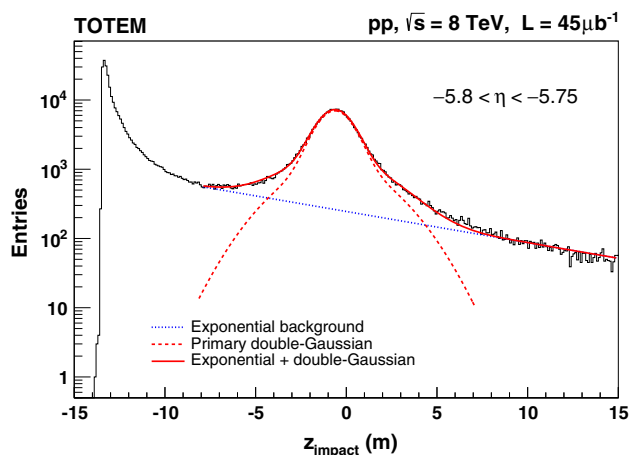


Fig. 2 The z_{impact} parameter distribution measured in the data, for tracks reconstructed in one T2 half-arm in the range $-5.8 < \eta < -5.75$. A global (double-Gaussian + exponential function) fit, performed in the range from -8 to 15 m is shown by the solid curve. The dotted curve represents the exponential component from secondary particles, while the dashed curve is the double-Gaussian component, mainly due to primary tracks

bin fit is performed for each η bin of the $dN_{\text{ch}}/d\eta$ distribution with the sum of a double-Gaussian and an exponential function, yielding standard deviations (amplitudes) of both Gaussian functions that increase (decrease) with η . The mean, required to be the same for both Gaussian distributions, the standard deviations and the amplitudes of the two Gaussian functions, as well as the mean and the amplitude of the exponential, are left free in the fit. The widths of the double-Gaussian distributions are consistent with the observed angular resolution of about 0.5 mrad for the T2 track reconstruction. The relative abundance of secondary particles is found to be smaller for higher $|\eta|$. The fit of the z_{impact} distribution is also repeated by using a second degree polynomial for the description of the background. The results are found to be stable with respect to the choice of the background function. The integral of the fitting function approximates the area of the z_{impact} distribution to within 1% .

The T2 tracks are considered “primary candidates” if they are in the z_{impact} range corresponding to 96% of the area of the double-Gaussian, taken symmetrically around the mean.

The standard CMS track reconstruction algorithm is based on a combinatorial track finder (CTF) [16]. The collection of reconstructed tracks is produced by multiple iterations of the CTF track reconstruction sequence, in a process called iterative tracking. The reconstruction of the interaction vertices in the event uses the available reconstructed track collection. Prompt tracks are selected based on given quality criteria, and the selected tracks are then clustered in z using a “deterministic annealing” (DA) algorithm [48]. After identifying candidate vertices based on the DA clustering, the candidates containing at least two tracks are fitted by means of an

adaptive vertex fit, where tracks in the vertex are assigned a weight between 0 and 1 based on their compatibility with the common vertex. In the central region, covered by the CMS tracker, high-purity primary tracks [49] are selected with $p_{\text{T}} > 0.1$ GeV/ c and relative p_{T} uncertainty less than 10% . To maximise the track-vertex association efficiency, a selection is applied on the track impact parameter, both along the z -axis and in the transverse plane. The impact parameter with respect to the beam spot in the transverse plane, d_{xy} , is required to be $|d_{xy}/\sigma_{xy}| < 3$, while for the point of closest approach to the primary vertex along the z -direction, d_z , the requirement $|d_z/\sigma_z| < 3$ is imposed. Here σ_{xy} and σ_z denote the uncertainties in d_{xy} and d_z , respectively. The analysis is restricted to $|\eta| < 2.2$, to avoid effects from tracks close to the geometric edge of the tracker. Events with more than one reconstructed vertex are discarded, thus reducing the effect of pileup to a negligible level ($< 1\%$).

The pseudorapidity distributions of the charged particles are measured in the central and forward regions for three different event samples, with topologies corresponding to three different event selection criteria. An inclusive sample of events is selected by requiring at least one primary-track candidate in T2. Event samples enhanced in non-single diffractive dissociation (NSD) and single diffractive dissociation (SD) events are also selected, the former defined by requiring a least one primary candidate in each of the two T2 telescopes and the latter by selecting events with at least one primary candidate in one T2 telescope and none in the other. Therefore, the intersection of the NSD-enhanced and SD-enhanced samples is empty, while the union is the inclusive sample.

The inclusive sample includes $\sim 99\%$ of non-diffractive events. The reconstruction efficiency for diffractive events is 50% for a diffractive mass $M \sim 3.6$ GeV/ c^2 and increases rapidly to 99% for $M > 10$ GeV/ c^2 . Most of the non-diffractive and double diffractive events, as well as the single diffractive events with masses larger than 1.3 TeV/ c^2 , produce particles in both T2 telescopes and are therefore included in the NSD-enhanced sample. Simulation studies based on PYTHIA8 and EPOS show that the fraction of NSD events in the SD-enhanced sample amounts to 45 – 65% .

6 Data analysis

The pseudorapidity density measurements presented here refer to “stable” primary charged particles, with an average lifetime longer than 3×10^{-11} s, either directly produced in pp collisions or from decays of particles with shorter lifetimes. Such a definition, consistent with that of previous studies [3–7, 9], considers as secondary particles the decay products of K_S^0 and Λ hadrons and all of the charged particles gener-

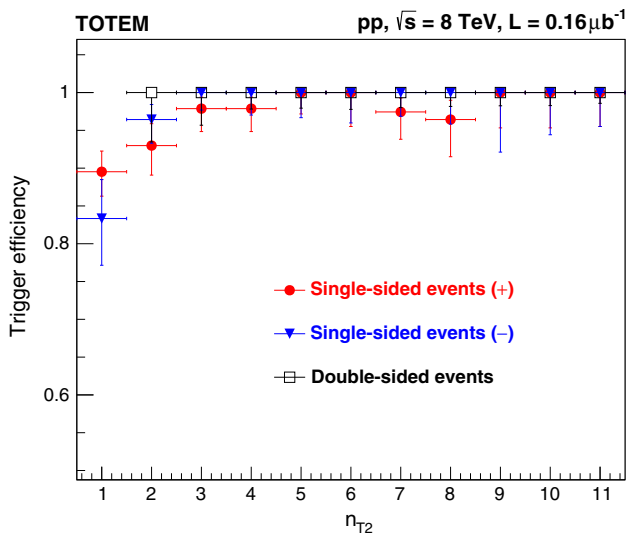


Fig. 3 Trigger efficiency as a function of the total track multiplicity in the T2 telescopes for single-sided events with primary candidates in only the $z > 0$ (+) or $z < 0$ (-) telescope and for double-sided events with primary candidates in both telescopes

ated by interactions with the material in front and around the detectors.

6.1 Trigger efficiency correction

The trigger efficiency is determined with a zero bias event sample separately for events with primary-track candidates reconstructed offline in both arms of T2 and in only one arm. All zero bias data taken were used to determine the trigger inefficiency. The inefficiency of the trigger is mainly due to non-operating and noisy channels. For each event category, the trigger efficiency is calculated as a function of the total number of tracks reconstructed offline in T2, n_{T2} , as $\epsilon_{\text{trig}} = N(n_{T2})_{\text{trig}}/N(n_{T2})_{\text{zb}}$, where $N(n_{T2})_{\text{trig}}$ is the number of events with the total T2 track multiplicity n_{T2} passing the trigger selection and $N(n_{T2})_{\text{zb}}$ is the number of events with n_{T2} tracks selected with the zero bias trigger. The measured trigger efficiency is shown in Fig. 3.

The trigger efficiency correction, $1/\epsilon_{\text{trig}}$, is applied separately for the three event categories and is significant for events with $n_{T2} = 1$, while it approaches unity for $n_{T2} \geq 3$. The overall trigger inefficiency results in a 0.1–0.2 % relative correction to the total $dN_{\text{ch}}/d\eta$ distributions for the three event categories. The value of the associated systematic uncertainty is conservatively assumed to be equal to this relative correction.

6.2 Event selection correction

In order to take into account the differences between the sample defined at the MC-particle level (“gen selected”) and

the one selected based on the reconstructed tracks (“reco selected”), a correction factor needs to be introduced. This correction is calculated for each η bin and event category from the ratio

$$C_{\text{sel}}(\eta) = \frac{dN_{\text{ch}}/d\eta_{\text{gen}}|_{\text{gen selected}}}{dN_{\text{ch}}/d\eta_{\text{gen}}|_{\text{reco selected}}}, \tag{1}$$

where the numerator is the pseudorapidity density obtained from the MC simulation for events selected based on the charged particles within the T2 acceptance, while the denominator is the density obtained by selecting the simulated events according to the topology of the primary candidates in T2, as explained in Sect. 5. In general, C_{sel} is different from unity because of migrations between the different event categories. Because of misidentification of secondary particles as primaries and of track reconstruction inefficiencies, an event can be classified (according to the configuration of its reconstructed tracks) in a category that does not reflect its true charged-particle content.

For the inclusive and NSD-enhanced analysis, C_{sel} is evaluated with PYTHIA8 and EPOS. Moreover, to quantify possible biases related to this correction, the analyses are repeated with the same selection method defined in Sect. 5 but without the primary candidate z_{impact} requirement.

As the SD-enhanced multiplicity is smaller than the NSD-enhanced multiplicity, a larger selection inefficiency is expected for the former class of events. Moreover, as the SD-enhanced sample represents only 26 % of the inclusive sample, the NSD events that are wrongly identified as SD can introduce a large bias in the measured SD-enhanced $dN_{\text{ch}}/d\eta$ distributions. Additional studies of the event selection strategy for the SD-enhanced analysis are therefore performed. The analysis is repeated with different event selection strategies and C_{sel} is reevaluated for each as a function of η and of the track multiplicity in T2. The selection methods differ in the maximum number of tracks and of primary candidates reconstructed in T2 on each side of the IP. Simulation studies show that, depending on the method and the MC generator used, the selection efficiency is in the range of 70–90 %. The purity of the SD-enhanced sample, defined as the fraction of the selected events with primary charged particles in only one arm of T2, varies between 66 and 81 %. The dependence of the SD-enhanced $dN_{\text{ch}}/d\eta$ distributions on the selection methods is used to evaluate the systematic uncertainty related to the event selection. More details on the numerical values of C_{sel} are given in Sects. 6.3 and 6.4.

6.3 Measurement of $dN_{\text{ch}}/d\eta$ in the central region

The charged-particle pseudorapidity distributions in the central region are obtained from the raw distributions of charged tracks after applying a number of corrections according to the formula:

$$\frac{dN_{ch}}{d\eta} = \frac{C_{sel}(\eta) \sum_{evt} \omega_{evt}(n_{CMS}, n_{T2}) \sum_{trk \in S} \omega_{trk}(n_{CMS}, p_T, \eta)}{\Delta\eta \sum_{n_{CMS}} N_{evt}(n_{CMS}, n_{T2}) \omega_{evt}(n_{CMS}, n_{T2})}, \tag{2}$$

where S is the sample of tracks that pass the selection criteria for a given η bin, n_{CMS} and n_{T2} is the total number of reconstructed tracks in the CMS tracker and T2, respectively, N_{evt} is the number of triggered events in the corresponding track multiplicity bins, ω_{evt} corrects for the trigger and the vertex reconstruction efficiencies, ω_{trk} corrects for the tracking efficiency and the effect of non-primary tracks and C_{sel} corrects for the effect of the event and primary-track selection with T2. The bin width in η is $\Delta\eta = 0.2$.

The event correction, ω_{evt} , depends on the track multiplicity in T2, n_{T2} , as well as on the multiplicity in the CMS tracker because of the minimum number of tracks required in the vertex reconstruction. It is given by

$$\omega_{evt}(n_{CMS}, n_{T2}) = \frac{1}{\epsilon_{trig}(n_{T2})\epsilon_{vtx}(n_{CMS})}, \tag{3}$$

where ϵ_{trig} is the trigger efficiency (Fig. 3) and ϵ_{vtx} is the primary vertex reconstruction and selection efficiency, calculated with PYTHIA6 as the ratio of the number of reconstructed events satisfying the primary vertex selection to the total number of generated events.

The correction for the tracking efficiency and non-primary tracks, $\omega_{trk}(n_{CMS}, p_T, \eta)$, is defined as:

$$\omega_{trk}(n_{CMS}, p_T, \eta) = \frac{1 - f_{np}(n_{CMS}, p_T, \eta)}{\epsilon_{trk}(n_{CMS}, p_T, \eta) (1 + f_m(n_{CMS}, p_T, \eta))}. \tag{4}$$

Here, ϵ_{trk} corrects for the geometric detector acceptance and the reconstruction tracking efficiency; the correction factor f_{np} accounts for the fraction of non-primary tracks, i.e. secondary and misidentified tracks, while f_m corrects for the effect of single charged particles that are reconstructed multiple times. These quantities are obtained from a detector simulation in bins of n_{CMS} , p_T and η . The effect of bin migrations is found to be negligible. Reconstructed events are required to pass the event selection and the generated particles are matched to the reconstructed tracks by using spatial and momentum information.

The tracking efficiency, ϵ_{trk} , is determined as the ratio of the number of all reconstructed tracks that are matched to generated particles and satisfy the track selection criteria in an (n_{CMS}, p_T, η) bin to the number of generated primary charged particles in that bin. As shown in Fig. 4 (top), ϵ_{trk} approaches unity for tracks with $p_T > 0.5$ GeV/c and $|\eta| < 1.5$.

The correction for non-primary tracks, f_{np} , is estimated as the ratio of the number of reconstructed tracks not matched

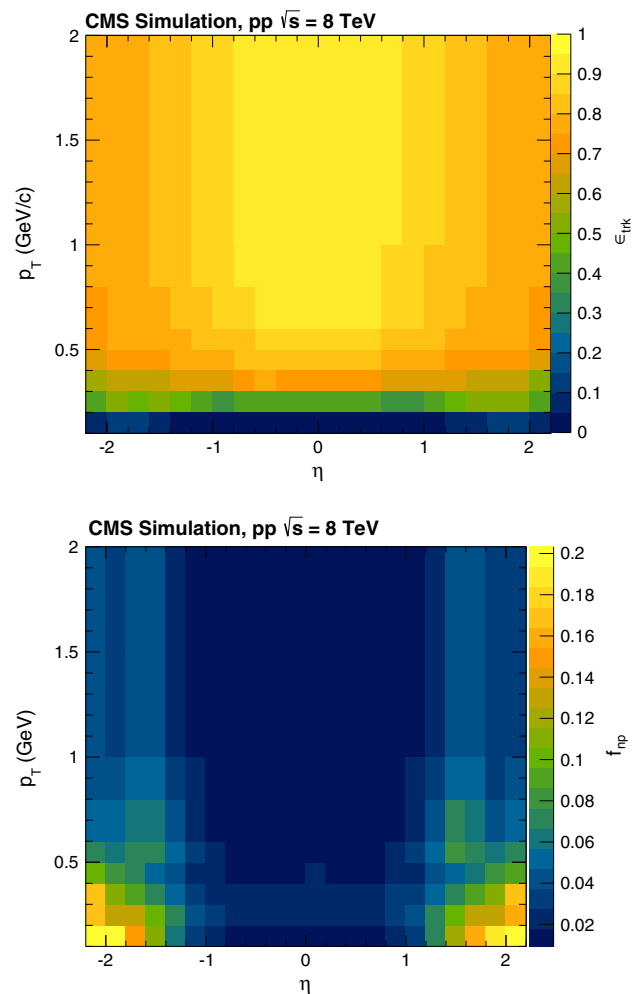


Fig. 4 Top Tracking efficiency, ϵ_{trk} , as a function of p_T and η and averaged over all multiplicity bins (n_{CMS}), for tracks with $p_T > 0.1$ GeV/c and $|\eta| < 2.2$. Bottom Correction factor, f_{np} , for non-primary tracks as a function of p_T and η and averaged over all multiplicity bins (n_{CMS}), for tracks with $p_T > 0.1$ GeV/c and $|\eta| < 2.2$

to a generated primary particle in a n_{CMS}, p_T, η bin to all reconstructed tracks in that bin. The correction varies as a function of η and p_T of the tracks, as shown in Fig. 4 (bottom), and reaches its lowest values of about 2 % for $|\eta| < 1.5$ and $p_T > 0.5$ GeV/c. It becomes as large as 20 % at very low transverse momentum ($p_T < 0.2$ GeV/c) and large pseudo-rapidity ($|\eta| > 1.8$).

The correction factor for multiply reconstructed particles, f_m , is estimated as the ratio of the number of generated primary charged particles that are associated to multiply reconstructed tracks in a given n_{CMS}, p_T, η bin to the number of generated charged particles in that bin. It is found to be below 1 %.

The model dependence of the corrections is determined by using PYTHIA6, EPOS and PYTHIA8. The corrected data, based on correction factors derived from each generator indepen-

Table 1 Systematic and statistical uncertainties of the $dN_{\text{ch}}/d\eta$ measurement in the central region. The given ranges indicate the η dependence of the uncertainties

Source	Inclusive (%)	NSD-enhanced (%)	SD-enhanced (%)
Event and primary-track selection ($C_{\text{sel}}(\eta)$)	3–5	4–6	9–16
Tracking efficiency	3.9	3.9	3.9
Trigger efficiency	0.1	0.1	0.1
Model dependence of track corrections (ω_{trk})	1–4	1–4	1–4
Correction to $p_T = 0$	0.2	0.2	0.2
Statistical	0.1	0.1	0.1
Total	5–7	6–8	10–17

dently, are found to differ by 1–4 % depending on the pseudorapidity bin. This amount is taken as a systematic uncertainty.

The average correction factor for the event selection, $C_{\text{sel}}(\eta)$, defined in Sect. 6.2, is found to be 1.01, 1.025, and 0.94 for the inclusive, NSD-enhanced and SD-enhanced samples, respectively, independent of pseudorapidity. The correction factor is obtained from EPOS and PYTHIA8. The average value of the correction factors from the two generators is applied to the data, while the relative difference between the two generators is taken as a systematic uncertainty. In addition, the event selection bias and the corresponding systematic uncertainty is estimated for each η bin as described in Sect. 6.2 by comparing the pseudorapidity distributions obtained with different methods. For the inclusive and NSD-enhanced samples, the systematic uncertainty in the event selection is found to be 3–5 and 4–6 %, respectively, while for the SD-enhanced sample it is 9–16 %.

Corrections of 4–6 % are applied to the final results to extrapolate to $p_T = 0$. The corrections are determined from the dN/dp_T spectrum of primary charged particles predicted by PYTHIA6 and PYTHIA8. The corrections obtained from the two MC generators differ by about 3 %, resulting in a systematic uncertainty in the $dN_{\text{ch}}/d\eta$ distributions of about 0.2 %. The same corrections are also estimated from Tsallis fits [50] to the p_T distributions for each η bin, giving consistent results.

A summary of the systematic uncertainties is given in Table 1. The uncertainties associated with the tracking efficiency are treated as uncorrelated between the η bins. For the inclusive and the NSD-enhanced samples, the most significant systematic uncertainties are those due to the uncertainty in the tracking efficiency and the event selection. The model dependence of C_{sel} and the uncertainty in the event selection are dominant for the SD-enhanced sample. The total uncertainty in the tracking efficiency is estimated to be 3.9 % from a comparison of two-body and four-body D^0 decays in data and simulated samples [51]. The uncertainties related to the primary vertex selection, the trigger efficiency and pileup events are found to be around 0.1 % and are neglected.

6.4 Measurement of $dN_{\text{ch}}/d\eta$ in the forward region

The pseudorapidity density in the forward region is measured for each T2 half-arm independently, thus providing a consistency check, as each half-arm differs in its alignment and track reconstruction efficiency. The number of primary-track candidates passing the z_{impact} parameter selection criteria is calculated for each η bin as a function of the z_{impact} -value with the double-Gaussian and exponential fits described in Sect. 5. The fraction of tracks associated to the double-Gaussian distribution core ranges from about 74 % (lower $|\eta|$ bins) to about 92 % (higher $|\eta|$ bins), and is used to weight each track by the probability for the track to be primary.

Each track is also weighted by the primary-track efficiency, which depends on η and on the average pad cluster multiplicity (APM) per plane in the corresponding half-arm. This efficiency, evaluated from MC generators, is defined as the probability to successfully reconstruct, with a z_{impact} parameter within the allowed region, a generated primary particle that falls within the acceptance of the detector. As shown in Fig. 5 for one of the T2 half-arms, the tracking efficiency decreases with increasing APM, since the reconstruction of tracks with sufficient number of hits becomes more difficult with larger occupancy. The average primary track efficiency ranges from about 73 % (lower $|\eta|$ bins) to about 87 % (higher $|\eta|$ bins), as shown in Fig. 5 for one of the T2 half-arms. The APM probability is a rapidly decreasing distribution, with average ~ 24 and RMS ~ 29 , for the inclusive selection. The rate of multiple associations of reconstructed tracks to the primary particle is negligible (<0.4 %) once the z_{impact} requirement is imposed.

Conversion of photons from π^0 decays in the material between the IP and T2, as well as decay products of strange particles, also contribute to the double-Gaussian peak. The overall non-primary contribution, to be subtracted from the double-Gaussian peak, was estimated as a function of η with PYTHIA8, EPOS and SIBYLL 2.1 [52]. The first two generators bracket the data in the forward region, while SIBYLL is introduced to also enclose the measurements from the LHCf

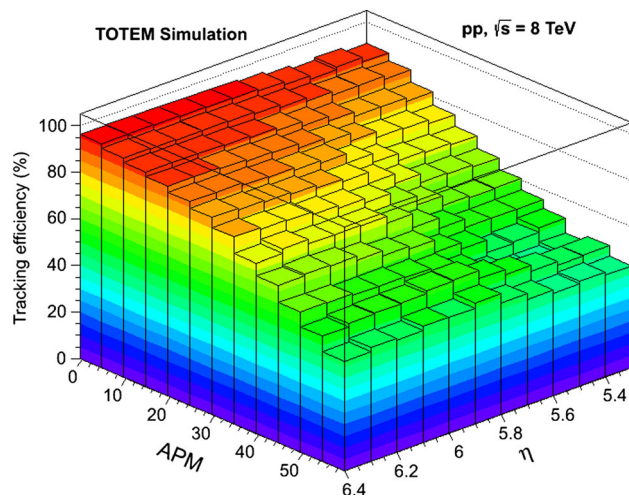


Fig. 5 Primary-track efficiency as a function of η and average pad cluster multiplicity (APM) in one T2 half-arm for the inclusive pp sample. The efficiency includes the track primary-candidate condition. Only particles with $p_T > 40$ MeV/c are considered

experiment of the photon dN/dE distribution [53]. The value of this correction is about 18 % and is obtained as the average of the three MC predictions.

The correction factors for the event selection bias ($C_{\text{sel}}(\eta)$) are about 1.05, 1.06 and 1.00 for the inclusive, NSD-enhanced and SD-enhanced event samples, respectively.

Bin migration effects in η are corrected for with PYTHIA8, which gives the best description of the slope of the measured $dN_{\text{ch}}/d\eta$ distribution. The effects are typically at the few percent level.

Events characterised by a high T2 hit multiplicity, typically due to showers generated by particles interacting with the material before T2, are not included in the analysis. These events, for which track reconstruction capability is limited, are characterised by an APM value larger than 60 and constitute 13.5, 16.5 and 6.3 % of the inclusive, NSD-enhanced and SD-enhanced samples, respectively. The effect of removing these events is evaluated in a MC study, which yields overall correction factors of about 1.05, 1.04 and 1.06 for the inclusive, NSD-enhanced and SD-enhanced samples, respectively. To verify the stability of this correction, the analysis is also repeated after excluding events with APM values larger than 45 and re-evaluating the corresponding MC corrections. The results of the two analyses agree within 1 %. In addition, this correction is also estimated by extrapolating the measured average multiplicity obtained as a function of the maximum APM included in the sample and without correcting for the missing fraction of the sample. The extrapolation, performed with a second degree polynomial, gives a correction that is within the MC uncertainty.

The fully corrected $dN_{\text{ch}}/d\eta$ distributions in each η bin are determined from:

$$\frac{dN_{\text{ch}}}{d\eta}(\eta_i) = \frac{2\pi}{\Delta\phi} \times \frac{C_{\text{sel}}(\eta_i) \sum_{\text{evt}} \omega_{\text{evt}}(n_{\text{T2}}) \sum_{\text{trk} \in S_j} B_{ij} \omega_{\text{trk}}(\text{APM}, \eta_j, z_{\text{impact}})}{\Delta\eta \sum_{n_{\text{T2}}} N_{\text{evt}}(n_{\text{T2}}) \omega_{\text{evt}}(n_{\text{T2}})}, \quad (5)$$

where S_j is the sample of tracks with $\eta_j - \Delta\eta/2 < \eta_j < \eta_j + \Delta\eta/2$ satisfying the selection criteria above, $\Delta\eta = 0.05$ is the bin width, C_{sel} is the correction factor related to the event selection defined in Sect. 6.2, B_{ij} is the bin migration correction associated with the j th bin in η . In addition, $\Delta\phi/2\pi = 192^\circ/360^\circ$ is the azimuthal acceptance of each T2 half-arm, $\omega_{\text{evt}}(n_{\text{T2}}) \equiv 1/\epsilon_{\text{trig}}(n_{\text{T2}})$ is the trigger efficiency correction, $N_{\text{evt}}(n_{\text{T2}})$ is the number of selected events with track multiplicity n_{T2} , and ω_{trk} is defined as:

$$\omega_{\text{trk}}(\text{APM}, \eta, z_{\text{impact}}) = \frac{P_{\text{prim}}(\eta, z_{\text{impact}}) S_{\text{np}}(\eta) C_{\text{mult}}(\eta)}{\epsilon(\eta, \text{APM})}, \quad (6)$$

where P_{prim} is the probability for a track to be primary. Here, ϵ is the primary-track efficiency, S_{np} is the correction factor for the non-primary contribution to the double-Gaussian peak and C_{mult} is the correction factor for the exclusion of events with APM values above 60.

The $dN_{\text{ch}}/d\eta$ distribution thus obtained refers to charged particles with $p_T > 40$ MeV/c, corresponding to the nominal p_T acceptance of T2. A MC-based estimation obtained with EPOS LHC and PYTHIA8 4C is used to correct the measurement down to $p_T = 0$. This correction, taken from the average of the two MC predictions, is about 2 %.

The evaluation of the systematic uncertainties for the $dN_{\text{ch}}/d\eta$ distributions is performed similarly to that discussed in [9]. Details are given in the following only for the most significant contributions.

The systematic uncertainty in the P_{prim} function, which is of order 4–5 %, is evaluated by including four effects: (a) the sensitivity to the misalignment corrections, quantified by varying the corrections within their uncertainties, (b) the sensitivity to the z_{impact} parameter fitting range, which was changed by either one or two meters depending on the η bin, (c) the sensitivity to the background parametrisation, obtained by replacing the exponential function with a second degree polynomial and (d) the difference between the area estimated by the fitting function and the integral of the z_{impact} distribution.

The systematic uncertainty in the primary-track efficiency is evaluated in studies where tracks are reconstructed with a set of five detector planes (out of the total of ten) in a single T2 half-arm. The track reconstruction efficiency is determined with the other set of detector planes in the same half-arm. The 5–6 % difference between the results obtained from simulation and from data is taken as an estimate of the systematic uncertainty.

Table 2 Systematic and statistical uncertainties of the $dN_{\text{ch}}/d\eta$ measurement with the T2 detector in the forward region. The first two contributions are half-arm dependent and partly η -uncorrelated, while the

remaining, excluding the statistical one, are half-arm independent and correlated across bins in η . The given ranges indicate the η dependence of the uncertainties

Source	Inclusive (%)	NSD-enhanced (%)	SD-enhanced (%)
Tracking efficiency data-MC discrepancy	5–6	5–6	5–6
Primary selection (including alignment)	4–5	4–5	4–5
Non-primaries in the double-Gaussian peak	5	5	5
Material effects	3–6	3–6	3–6
High-multiplicity events	3	3	3
Event selection	2–3	2–3	13–15
Tracking efficiency dependence on energy spectrum and magnetic field	2	2	2
Track quality criterion	1	1	1
Correction to $p_T = 0$	0.5	0.5	0.5
Trigger efficiency	0.2	0.2	0.2
Statistical	0.1	0.1	0.1
Total (after averaging half-arms)	10–12	10–12	16–18

The systematic uncertainty due to non-primary tracks included in the double-Gaussian once the exponential contribution has been removed, S_{np} , is evaluated by considering the range of the predictions of the EPOS, PYTHIA8 and SIBYLL MC generators, and is about 5 %.

The uncertainty in the correction for the exclusion of events with high secondary-particle multiplicity (C_{mult}) is taken as the difference between the EPOS and PYTHIA8 predictions, which is about 3 %. The uncertainty on the correction for the event selection (C_{sel}) is evaluated by taking into account both the dependence of the correction from the MCs mentioned above and the dependence of the $dN_{\text{ch}}/d\eta$ results on the different event selection strategies discussed earlier. This uncertainty is 13–15 % for the SD-enhanced sample and 2–3 % for the inclusive and NSD-enhanced samples.

The possible bias due to the material uncertainty and therefore on the production of secondary tracks is evaluated as a function of η from the MC vs. data discrepancy of the ratio between the number of tracks contained in the 96 % double-Gaussian area and all the tracks in the same range. The average discrepancy is in the range of 2–6 %. Simulation studies are also performed by varying the thickness of the material in front of T2 by 40 %. This part of the material is the main source of secondary tracks that contribute to the double-Gaussian. The effect of the change of the material results in a possible bias of less than 3 %.

Table 2 shows the uncertainties due to the corrections. To compute the total systematic uncertainty the errors are first separated into half-arm-correlated and uncorrelated parts and a weighted average between the four half-arms is taken. The $dN_{\text{ch}}/d\eta$ measurements obtained for the different T2 half-arms are found to be compatible.

The first two systematic uncertainties in Table 2 vary as a function of η and contribute to the uncorrelated bin-by-bin uncertainties. Conversely, the remaining systematic uncertainties affect all η bins in the same direction. The effect that systematic uncertainties might introduce in the difference of the $dN_{\text{ch}}/d\eta$ values at the beginning and at the end of the T2 acceptance is estimated to be at most 7 %.

The total uncertainty is obtained by adding in quadrature the η -correlated uncertainty and the η -uncorrelated one and the (negligible) statistical uncertainty.

7 Results

The combined CMS-TOTEM charged-particle pseudorapidity distributions are presented in Fig. 6 for the three event selection samples shown in Table 3. The results are derived in the central region by averaging the data points in the corresponding $\pm\eta$ bins and in the forward region by averaging over the four T2 half-arms. The uncertainty band represents the total uncertainty, while the bars show the statistical and uncorrelated systematics between neighbouring bins.

In the central region, the pseudorapidity density at $\eta = 0$ is 5.35 ± 0.36 for the inclusive sample, 6.20 ± 0.46 for the NSD-enhanced sample and $1.94^{+0.26}_{-0.23}$ for the SD-enhanced sample, with negligible statistical uncertainties. The predictions from various MC event generators differ from the data by up to 20 % for the inclusive and NSD-enhanced samples, with even larger discrepancies for the SD-enhanced sample. The data are well described by PYTHIA6 and QGSJETII-04 for the inclusive selection. For the NSD-enhanced sample, the predictions obtained from PYTHIA6 and QGSJETII-04 agree with the data for most η bins. A good description of the mea-

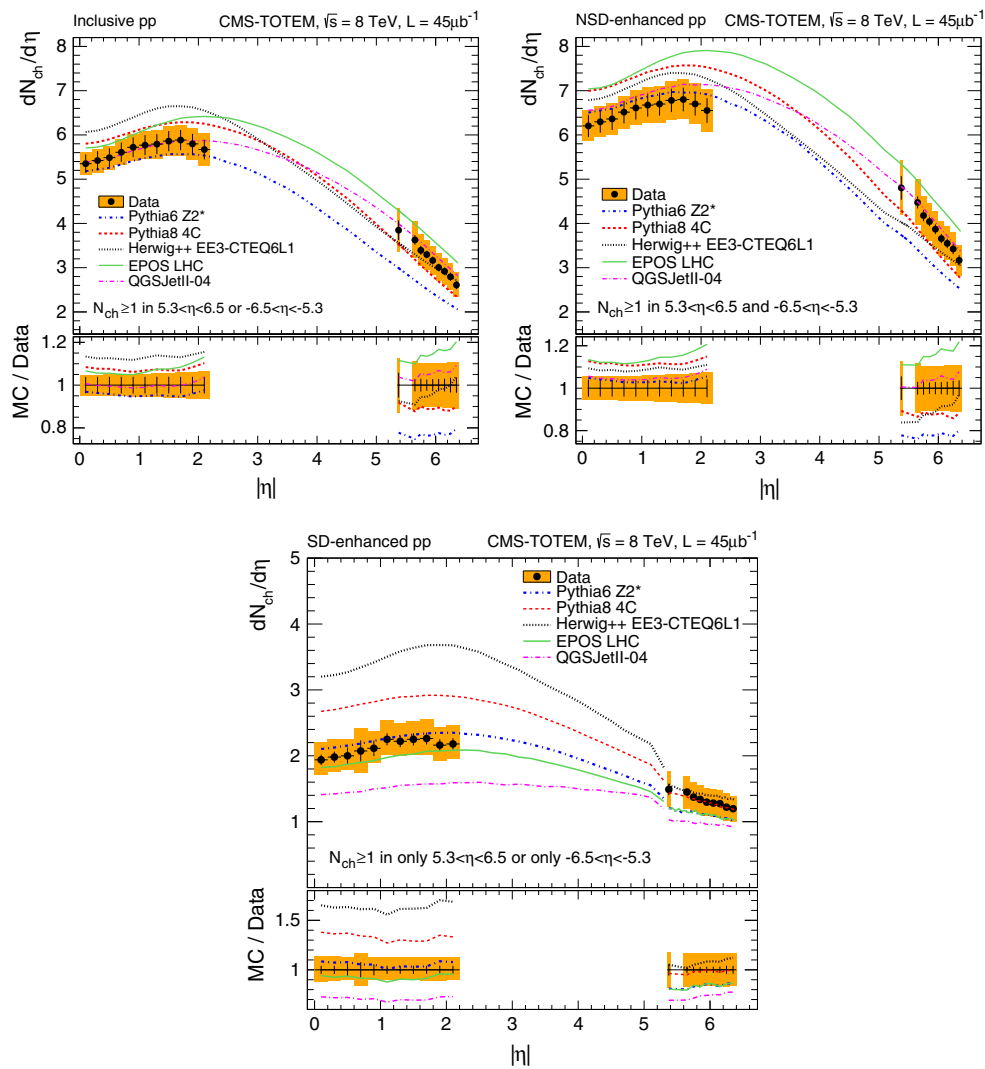


Fig. 6 Charged-particle pseudorapidity distributions from an inclusive sample (top left), a NSD-enhanced sample (top right), and a SD-enhanced sample (bottom). The error bars represent the statistical + uncorrelated systematics between neighbouring bins and the bands

show the combined systematic and statistical uncertainties. The measurements are compared to results from PYTHIA6, tune Z2*, PYTHIA8, tune 4C, HERWIG++, tune UE-EE-3 with CTEQ6L1 PDFs, EPOS, tune LHC and QGSJETII-04

Table 3 Event selection criteria applied at the stable-particle level in the MC simulation

Inclusive sample					
$N_{\text{charged particles}} > 0$	in	$5.3 < \eta < 6.5$	or	$-6.5 < \eta < -5.3$,	$p_T > 0$
NSD-enhanced sample					
$N_{\text{charged particles}} > 0$	in	$5.3 < \eta < 6.5$	and	$-6.5 < \eta < -5.3$,	$p_T > 0$
SD-enhanced sample					
$N_{\text{charged particles}} > 0$	in only	$5.3 < \eta < 6.5$	or only in	$-6.5 < \eta < -5.3$,	$p_T > 0$

surement for the SD-enhanced sample is provided by both EPOS and PYTHIA6.

The forward pseudorapidity density decreases with $|\eta|$. In the inclusive sample, $dN_{\text{ch}}/d\eta$ is 3.85 ± 0.49 at $\eta = 5.375$ and 2.61 ± 0.28 at $\eta = 6.350$, with negligible statistical uncertainty. The pseudorapidity density of the

NSD-enhanced sample ranges between 4.80 ± 0.62 and 3.17 ± 0.35 , while for the SD-enhanced sample it is in the range of 1.49 ± 0.27 to 1.20 ± 0.20 . The MC predictions for the three samples differ from the data by up to about $\pm 30\%$. For the inclusive and NSD-enhanced samples, the data in the forward region are in agreement with

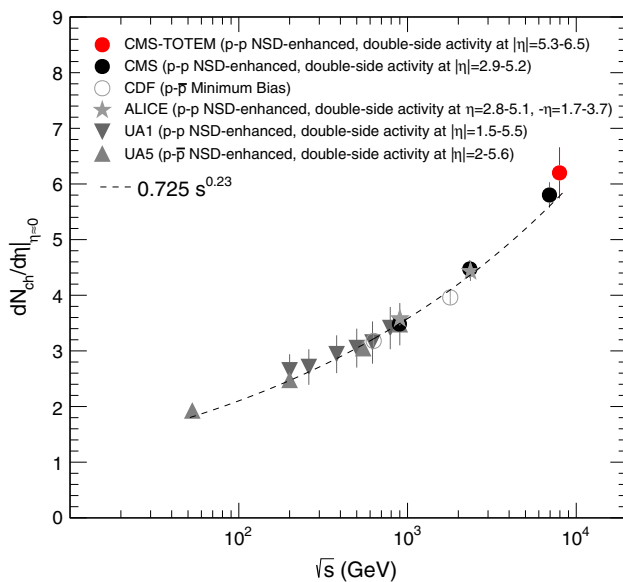


Fig. 7 Value of $dN_{\text{ch}}/d\eta|_{\eta=0}$ as a function of the centre-of-mass energy in pp and $p\bar{p}$ collisions. Shown are measurements performed with different NSD event selections from UA1 [12], UA5 [14], CDF [10, 11], ALICE [6] and CMS [4]. The dashed line is a power-law fit to the data

the prediction from QGSJETII-04 and are between the EPOS and PYTHIA8 results. For the SD-enhanced selection, the TOTEM data points are close to the PYTHIA8 and HERWIG++ predictions, while QGSJETII-04 underestimates the data. The change in the slope of the MC curves close to $\eta = 5.3$, more visible for the NSD- and SD-enhanced distributions, is due to the event selection requirement of at least one charged particle in the pseudorapidity region of T2.

The centre-of-mass energy dependence of the pseudorapidity distribution at $\eta \approx 0$ is shown in Fig. 7, which includes data from various other experiments for NSD events in pp and $p\bar{p}$ collisions. Although the different experiments do not use identical event selection criteria, they all include a large fraction of NSD events. Particle production at $\eta \approx 0$ is expected to follow a power-law dependence, $dN_{\text{ch}}/d\eta|_{\eta=0} \propto s^\epsilon$, with ϵ in the range 0.14–0.24 [40]. The result of fitting the high-energy pp and $p\bar{p}$ central-pseudorapidity particle densities with this function is shown in Fig. 7. A value of $\epsilon = 0.23 \pm 0.01$ is obtained.

8 Summary

Measurements of charged-particle densities over a large pseudorapidity range are presented for proton–proton (pp) collisions at a centre-of-mass energy of 8 TeV. The data were collected concurrently with the CMS and TOTEM detectors during a dedicated run with low probability for overlapping pp interactions in the same bunch crossing and correspond

to an integrated luminosity of $\mathcal{L} = 45 \mu\text{b}^{-1}$. Pseudorapidity distributions of charged particles within $|\eta| < 2.2$ and $5.3 < |\eta| < 6.4$ have been measured for three event samples with different final state topologies: a sample of inclusive inelastic pp events, a sample dominated by non-single diffractive dissociation (NSD) events and a sample enriched in single diffractive dissociation (SD) events. The data are compared to theoretical predictions obtained from five different MC event generators and tunes (PYTHIA6 Z2*, PYTHIA8 4C, HERWIG++ UE-EE-3, EPOS LHC tune, and QGSJETII-04).

In the central region, the inclusive and NSD-enhanced samples are well described by PYTHIA6 and QGSJETII. For the SD-enhanced sample a good description of the data is provided by both PYTHIA6 and EPOS. In the forward region, the pseudorapidity distributions for the inclusive and NSD-enhanced samples are between the PYTHIA8 and EPOS predictions. The QGSJETII predictions are compatible with the data. The pseudorapidity distribution in the SD-enhanced sample, affected by a larger systematic uncertainty, is best described by PYTHIA8 and HERWIG++.

The charged-particle densities obtained in this paper span the largest pseudorapidity interval ever measured at the LHC and have the unique potential to probe the correlation between particle production in the central region and that in the forward region. With the tunes used, none of the MC event generators are able to consistently describe the data over the whole η region and for all event samples.

Acknowledgments We congratulate our colleagues in the CERN accelerator departments for the excellent performance of the LHC. We especially thank the beam optics development team for the design and the successful commissioning of the high β -optics and the LHC machine coordinators for scheduling the dedicated fills. We are grateful to the technical and administrative staffs at CERN and at other CMS and TOTEM institutes for their contributions to the success of the CMS and TOTEM efforts. In addition, we gratefully acknowledge the computing centres and personnel of the Worldwide LHC Computing Grid for delivering so effectively the computing infrastructure essential to our analyses. We acknowledge the enduring support for the construction and operation of the LHC and the CMS and TOTEM detectors provided by our affiliated institutions as included in the lists of authors and the following funding agencies: the Austrian Federal Ministry of Science, Research and Economy and the Austrian Science Fund; the Belgian Fonds de la Recherche Scientifique and Fonds voor Wetenschappelijk Onderzoek; the Brazilian Funding Agencies (CNPq, CAPES, FAPERJ and FAPESP); the Bulgarian Ministry of Education, Youth and Science; CERN; the Chinese Academy of Sciences, Ministry of Science and Technology and National Natural Science Foundation of China; the Colombian Funding Agency (COLCIENCIAS); the Croatian Ministry of Science, Education and Sport and the Croatian Science Foundation; the Research Promotion Foundation, Cyprus; the Ministry of Education and Research, Estonian Research Council via IUT23-4 and IUT23-6 and European Regional Development Fund, Estonia; the Academy of Finland, Finnish Ministry of Education and Culture and Helsinki Institute of Physics; the Institut National de Physique Nucléaire et de Physique des Particules / CNRS and Commissariat à l'Énergie Atomique et aux Énergies Alternatives / CEA, France; the Bundesministerium für Bildung und Forschung, Deutsche Forschungs-

gemeinschaft and Helmholtz-Gemeinschaft Deutscher Forschungszentren, Germany; the General Secretariat for Research and Technology, Greece; the National Scientific Research Foundation, National Innovation Office and the OTKA Grant NK 101438, 73143, Hungary; the Department of Atomic Energy and the Department of Science and Technology, India; the Institute for Studies in Theoretical Physics and Mathematics, Iran; the Science Foundation, Ireland; the Istituto Nazionale di Fisica Nucleare, Italy; the Korean Ministry of Education, Science and Technology and the World Class University program of NRF, Republic of Korea; the Lithuanian Academy of Sciences; the Ministry of Education and University of Malaya (Malaysia); the Mexican Funding Agencies (CINVESTAV, CONACYT, SEP and UASLP-FAI); the Ministry of Business, Innovation and Employment, New Zealand; the Pakistan Atomic Energy Commission; the Ministry of Science and Higher Education and the National Science Centre, Poland; the Fundação para a Ciência e a Tecnologia, Portugal; JINR (Armenia, Belarus, Georgia, Ukraine, Uzbekistan); the Ministry of Education and Science of the Russian Federation, the Federal Agency of Atomic Energy of the Russian Federation, Russian Academy of Sciences and the Russian Foundation for Basic Research; the Ministry of Education, Science and Technological Development of Serbia; the Secretaría de Estado de Investigación, Desarrollo e Innovación and Programa Consolider-Ingenio 2010, Spain; the Swiss Funding Agencies (ETH Board, ETH Zurich, PSI, SNF, UniZH, Canton Zurich and SER); the Ministry of Science and Technology, Taipei; the Thailand Center of Excellence in Physics, the Institute for the Promotion of Teaching Science and Technology of Thailand, Special Task Force for Activating Research and the National Science and Technology Development Agency of Thailand; the Scientific and Technical Research Council of Turkey and Turkish Atomic Energy Authority; the National Academy of Sciences of Ukraine and State Fund for Fundamental Researches, Ukraine; the Science and Technology Facilities Council, UK; the US Department of Energy and the US National Science Foundation. Individuals have received support from the Marie-Curie programme and the European Research Council and EPLANET (European Union); the Leventis Foundation; the A. P. Sloan Foundation; the Alexander von Humboldt Foundation; the Belgian Federal Science Policy Office; the Fonds pour la Formation à la Recherche dans l'Industrie et dans l'Agriculture (FRIA-Belgium); the Agentschap voor Innovatie door Wetenschap en Technologie (IWT-Belgium); the Ministry of Education, Youth and Sports (MEYS) of the Czech Republic; the Magnus Ehrnrooth foundation and the Waldemar von Frenckell foundation, Finland; the Finnish Academy of Science and Letters (The Vilho, Yrjö and Kalle Väisälä Fund) and the Charles Simonyi Fund (Hungary); the Council of Science and Industrial Research, India; the Compagnia di San Paolo (Torino); the HOMING PLUS programme of Foundation for Polish Science, cofinanced by EU, Regional Development Fund; and the Thalís and Aristeia programmes cofinanced by EU-ESF and the Greek NSRF.

Open Access This article is distributed under the terms of the Creative Commons Attribution License which permits any use, distribution, and reproduction in any medium, provided the original author(s) and the source are credited.
Funded by SCOAP³ / License Version CC BY 4.0.

References

1. S. Ostapchenko, On the model dependence of the relation between minimum-bias and inelastic proton-proton cross sections. *Phys. Lett. B* **703**, 588 (2011). doi:[10.1016/j.physletb.2011.08.050](https://doi.org/10.1016/j.physletb.2011.08.050). arXiv:[1103.5684](https://arxiv.org/abs/1103.5684)
2. ALICE Collaboration, Measurement of inelastic, single- and double-diffraction cross sections in proton–proton collisions at the LHC with ALICE. *Eur. Phys. J. C* **73**, 2456 (2013). doi:[10.1140/epjc/s10052-013-2456-0](https://doi.org/10.1140/epjc/s10052-013-2456-0). arXiv:[1208.4968](https://arxiv.org/abs/1208.4968)
3. CMS Collaboration, Transverse momentum and pseudorapidity distributions of charged hadrons in pp collisions at $\sqrt{s} = 0.9$ and 2.36 TeV. *JHEP* **02**, 041 (2010). doi:[10.1007/JHEP02\(2010\)041](https://doi.org/10.1007/JHEP02(2010)041)
4. CMS Collaboration, Transverse-momentum and pseudorapidity distributions of charged hadrons in pp collisions at $\sqrt{s} = 7$ TeV. *Phys. Rev. Lett.* **105**, 022002 (2010). doi:[10.1103/PhysRevLett.105.022002](https://doi.org/10.1103/PhysRevLett.105.022002)
5. ATLAS Collaboration, Charged-particle multiplicities in pp interactions measured with the ATLAS detector at the LHC. *New J. Phys.* **13**, 053033 (2011). doi:[10.1088/1367-2630/13/5/053033](https://doi.org/10.1088/1367-2630/13/5/053033)
6. ALICE Collaboration, Charged-particle multiplicity measurement in proton–proton collisions at $\sqrt{s} = 0.9$ and 2.36 TeV with ALICE at LHC. *Eur. Phys. J. C* **68**, 89 (2010). doi:[10.1140/epjc/s10052-010-1339-x](https://doi.org/10.1140/epjc/s10052-010-1339-x)
7. ALICE Collaboration, Charged-particle multiplicity measurement in proton–proton collisions at $\sqrt{s} = 7$ TeV with ALICE at LHC. *Eur. Phys. J. C* **68**, 345 (2010). doi:[10.1140/epjc/s10052-010-1350-2](https://doi.org/10.1140/epjc/s10052-010-1350-2)
8. LHCb Collaboration, Measurement of charged particle multiplicities in pp collisions at $\sqrt{s} = 7$ TeV in the forward region. *Eur. Phys. J. C* **72**, 1947 (2012). doi:[10.1140/epjc/s10052-012-1947-8](https://doi.org/10.1140/epjc/s10052-012-1947-8)
9. TOTEM Collaboration, Measurement of the forward charged-particle pseudorapidity density in pp collisions at $\sqrt{s} = 7$ TeV with the TOTEM experiment. *Europhys. Lett.* **98**, 31002 (2012). doi:[10.1209/0295-5075/98/31002](https://doi.org/10.1209/0295-5075/98/31002)
10. CDF Collaboration, Measurement of particle production and inclusive differential cross sections in $p\bar{p}$ collisions at $\sqrt{s} = 1.96$ TeV. *Phys. Rev. D* **79**, 112005 (2009). doi:[10.1103/PhysRevD.79.112005](https://doi.org/10.1103/PhysRevD.79.112005) [Erratum doi:[10.1103/PhysRevD.82.119903](https://doi.org/10.1103/PhysRevD.82.119903)]
11. CDF Collaboration, Pseudorapidity distributions of charged particles produced in $p\bar{p}$ interactions at $\sqrt{s} = 630$ GeV and 1800 GeV. *Phys. Rev. D* **41**, 2330 (1990). doi:[10.1103/PhysRevD.41.2330](https://doi.org/10.1103/PhysRevD.41.2330)
12. UA1 Collaboration, A study of the general characteristics of proton–antiproton collisions at $\sqrt{s} = 0.2$ to 0.9 TeV. *Nucl. Phys. B* **335**, 261 (1990). doi:[10.1016/0550-3213\(90\)90493-W](https://doi.org/10.1016/0550-3213(90)90493-W)
13. UA4 Collaboration, Pseudorapidity distribution of charged particles in diffraction dissociation events at the CERN SPS collider. *Phys. Lett. B* **166**, 459 (1986). doi:[10.1016/0370-2693\(86\)91598-4](https://doi.org/10.1016/0370-2693(86)91598-4)
14. UA5 Collaboration, Scaling of pseudorapidity distributions at c.m. energies up to 0.9 TeV. *Z. Phys. C* **33**, 1 (1986). doi:[10.1007/BF01410446](https://doi.org/10.1007/BF01410446)
15. CMS Collaboration, The CMS experiment at the CERN LHC. *JINST* **3**, S08004 (2008). doi:[10.1088/1748-0221/3/08/S08004](https://doi.org/10.1088/1748-0221/3/08/S08004)
16. CMS Collaboration, Track and vertex reconstruction in CMS. *Nucl. Instrum. Methods A* **582**, 781 (2007). doi:[10.1016/j.nima.2007.07.091](https://doi.org/10.1016/j.nima.2007.07.091)
17. TOTEM Collaboration, The TOTEM experiment at the CERN large hadron collider. *JINST* **3**, S08007 (2008). doi:[10.1088/1748-0221/3/08/S08007](https://doi.org/10.1088/1748-0221/3/08/S08007)
18. TOTEM Collaboration, Performance of the TOTEM detectors at the LHC. *Int. J. Mod. Phys. A* **28**, 1330046 (2013). doi:[10.1142/S0217751X13300469](https://doi.org/10.1142/S0217751X13300469). arXiv:[1310.2908](https://arxiv.org/abs/1310.2908)
19. M. Bagliesi et al., The TOTEM T2 telescope based on triple-GEM chambers. *Nucl. Instrum. Methods A* **617**, 134 (2010). doi:[10.1016/j.nima.2009.07.006](https://doi.org/10.1016/j.nima.2009.07.006)
20. M. Berretti, Measurement of the forward charged particle pseudorapidity density in pp collisions at $\sqrt{s} = 7$ TeV with the TOTEM experiment. PhD thesis, Siena, 2012. CERN-THESIS-2012-231, chap. 3
21. GEANT4 Collaboration, GEANT4—a simulation toolkit. *Nucl. Instrum. Methods A* **506**, 250 (2003). doi:[10.1016/S0168-9002\(03\)01368-8](https://doi.org/10.1016/S0168-9002(03)01368-8)
22. T. Sjöstrand, S. Mrenna, P. Skands, PYTHIA 6.4 physics and manual. *JHEP* **05**, 026 (2006). doi:[10.1088/1126-6708/2006/05/026](https://doi.org/10.1088/1126-6708/2006/05/026)

23. T. Sjöstrand, S. Mrenna, P. Skands, A brief introduction to PYTHIA 8.1. *Comput. Phys. Commun.* **178**, 852 (2008). doi:[10.1016/j.cpc.2008.01.036](https://doi.org/10.1016/j.cpc.2008.01.036)
24. R. Corke, T. Sjöstrand, Interleaved parton showers and tuning prospects. *JHEP* **03**, 032 (2011). doi:[10.1007/JHEP03\(2011\)032](https://doi.org/10.1007/JHEP03(2011)032). arXiv:[1011.1759](https://arxiv.org/abs/1011.1759)
25. P. Skands, D. Wicke, Non-perturbative QCD effects and the top mass at the Tevatron. *Eur. Phys. J. C* **52**, 133 (2007). doi:[10.1140/epjc/s10052-007-0352-1](https://doi.org/10.1140/epjc/s10052-007-0352-1)
26. CMS Collaboration, Measurement of energy flow at large pseudorapidities in pp collisions at $\sqrt{s} = 0.9$ and 7 TeV. *JHEP* **11**, 148 (2011). doi:[10.1007/JHEP11\(2011\)148](https://doi.org/10.1007/JHEP11(2011)148). arXiv:[1110.0211](https://arxiv.org/abs/1110.0211) [Erratum doi:[10.1007/JHEP02\(2012\)055](https://doi.org/10.1007/JHEP02(2012)055)]
27. Pumplin et al., New generation of parton distributions with uncertainties from global QCD analysis. *JHEP* **07**, 012 (2002). doi:[10.1088/1126-6708/2002/07/012](https://doi.org/10.1088/1126-6708/2002/07/012). arXiv:[hep-ph/0201195](https://arxiv.org/abs/hep-ph/0201195)
28. V.N. Gribov, L.N. Lipatov, Deep inelastic $e p$ scattering in perturbation theory. *Sov. J. Nucl. Phys.* **15**, 438 (1972)
29. G. Altarelli, G. Parisi, Asymptotic freedom in parton language. *Nucl. Phys. B* **126**, 298 (1977). doi:[10.1016/0550-3213\(77\)90384-4](https://doi.org/10.1016/0550-3213(77)90384-4)
30. Y.L. Dokshitzer, Calculation of the structure functions for deep inelastic scattering and $e^+ e^-$ annihilation by perturbation theory in quantum chromodynamics. *Sov. Phys. JETP* **46**, 641 (1977)
31. B. Andersson, G. Gustafson, G. Ingelman, T. Sjöstrand, Parton fragmentation and string dynamics. *Phys. Rep.* **97**, 31 (1983). doi:[10.1016/0370-1573\(83\)90080-7](https://doi.org/10.1016/0370-1573(83)90080-7)
32. G.A. Schuler, T. Sjöstrand, Hadronic diffractive cross sections and the rise of the total cross section. *Phys. Rev. D* **49**, 2257 (1994). doi:[10.1103/PhysRevD.49.2257](https://doi.org/10.1103/PhysRevD.49.2257)
33. H1 Collaboration, Measurement and QCD analysis of the diffractive deep-inelastic scattering cross-section at HERA. *Eur. Phys. J. C* **48**, 715 (2006). doi:[10.1140/epjc/s10052-006-0035-3](https://doi.org/10.1140/epjc/s10052-006-0035-3). arXiv:[hep-ex/0606004](https://arxiv.org/abs/hep-ex/0606004)
34. H1 Collaboration, Dijet cross sections and parton densities in diffractive DIS at HERA. *JHEP* **10**, 042 (2007). doi:[10.1088/1126-6708/2007/10/042](https://doi.org/10.1088/1126-6708/2007/10/042). arXiv:[0708.3217](https://arxiv.org/abs/0708.3217)
35. P. Newman, M. Wing, The hadronic final state at HERA (2013). *Rev. Mod. Phys.* **86**, 1037 (2014). doi:[10.1103/RevModPhys.86.1037](https://doi.org/10.1103/RevModPhys.86.1037). arXiv:[1308.3368](https://arxiv.org/abs/1308.3368)
36. S. Navin, Diffraction in PYTHIA. LUTP-09-23, MCnet/10/09 (2010). arXiv:[1005.3894](https://arxiv.org/abs/1005.3894)
37. M. Bähr et al., Herwig++ physics and manual. *Eur. Phys. J. C* **58**, 639 (2008). doi:[10.1140/epjc/s10052-008-0798-9](https://doi.org/10.1140/epjc/s10052-008-0798-9)
38. S. Gieseke, C. Röhr, A. Siódmok, Colour reconnections in Herwig++. *Eur. Phys. J. C* **72**, 2225 (2012). doi:[10.1140/epjc/s10052-012-2225-5](https://doi.org/10.1140/epjc/s10052-012-2225-5). arXiv:[1206.0041](https://arxiv.org/abs/1206.0041)
39. S. Gieseke et al., Herwig++ 2.5 release note. DCPT/11/18, DESY 11-018, IPPP/11/09, KA-TP-04-2011, MCnet-11-04 (2011). arXiv:[1102.1672](https://arxiv.org/abs/1102.1672)
40. D. d'Enterria, R. Engel, T. Pierog, S. Ostapchenko, K. Werner, Constraints from the first LHC data on hadronic event generators for ultra-high energy cosmic-ray physics. *Astropart. Phys.* **35**, 98 (2011). doi:[10.1016/j.astropartphys.2011.05.002](https://doi.org/10.1016/j.astropartphys.2011.05.002). arXiv:[1101.5596](https://arxiv.org/abs/1101.5596)
41. K. Werner, F.M. Liu, T. Pierog, Parton ladder splitting and the rapidity dependence of transverse momentum spectra in deuteron-gold collisions at RHIC. *Phys. Rev. C* **74**, 044902 (2006). doi:[10.1103/PhysRevC.74.044902](https://doi.org/10.1103/PhysRevC.74.044902). arXiv:[hep-ph/0506232](https://arxiv.org/abs/hep-ph/0506232)
42. T. Pierog et al., EPOS LHC: test of collective hadronization with LHC data (2013). arXiv:[1306.0121](https://arxiv.org/abs/1306.0121)
43. S. Ostapchenko, Monte Carlo treatment of hadronic interactions in enhanced Pomeron scheme: I. QGSJET-II model. *Phys. Rev. D* **83**, 014018 (2011). doi:[10.1103/PhysRevD.83.014018](https://doi.org/10.1103/PhysRevD.83.014018)
44. V.N. Gribov, A Reggeon diagram technique. *Sov. Phys. JETP* **26**, 414 (1968)
45. T. Pierog, LHC results and high energy cosmic ray interaction models. *J. Phys. Conf. Ser.* **409**, 012008 (2013). doi:[10.1088/1742-6596/409/1/012008](https://doi.org/10.1088/1742-6596/409/1/012008)
46. TOTEM Collaboration, Measurement of proton-proton inelastic scattering cross-section at $\sqrt{s} = 7$ TeV. *Europhys. Lett.* **101**, 21003 (2013). doi:[10.1209/0295-5075/101/21003](https://doi.org/10.1209/0295-5075/101/21003)
47. TOTEM Collaboration, Luminosity-independent measurement of the proton-proton total cross section at $\sqrt{s} = 8$ TeV. *Phys. Rev. Lett.* **111**, 012001 (2013). doi:[10.1103/PhysRevLett.111.012001](https://doi.org/10.1103/PhysRevLett.111.012001)
48. K. Rose, Deterministic annealing for clustering, compression, classification, regression, and related optimization problems. *Proc. IEEE* **86**(11), 2210 (1998). doi:[10.1109/5.726788](https://doi.org/10.1109/5.726788)
49. CMS Collaboration, Tracking and vertexing results from first collisions. CMS Physics Analysis Summary CMS-PAS-TRK-10-001 (2010)
50. C. Tsallis, Possible generalization of Boltzmann-Gibbs statistics. *J. Stat. Phys.* **52**, 479 (1988). doi:[10.1007/BF01016429](https://doi.org/10.1007/BF01016429)
51. CMS Collaboration, Measurement of tracking efficiency. CMS Physics Analysis Summary CMS-PAS-TRK-10-002 (2010)
52. E.-J. Ahn et al., Cosmic ray interaction event generator SIBYLL 2.1. *Phys. Rev. D* **80**, 094003 (2009). doi:[10.1103/PhysRevD.80.094003](https://doi.org/10.1103/PhysRevD.80.094003). arXiv:[0906.4113](https://arxiv.org/abs/0906.4113)
53. LHCf Collaboration, Measurement of zero degree single photon energy spectra for $\sqrt{s} = 7$ TeV proton-proton collisions at LHC. *Phys. Lett. B* **703**, 128 (2011). doi:[10.1016/j.physletb.2011.07.077](https://doi.org/10.1016/j.physletb.2011.07.077). arXiv:[1104.5294](https://arxiv.org/abs/1104.5294)

The CMS Collaboration

Yerevan Physics Institute, Yerevan, Armenia

S. Chatrchyan, V. Khachatryan, A. M. Sirunyan, A. Tumasyan

Institut für Hochenergiephysik der OeAW, Vienna, Austria

W. Adam, T. Bergauer, M. Dragicevic, J. Erö, C. Fabjan¹, M. Friedl, R. Frühwirth¹, V. M. Ghete, C. Hartl, N. Hörmann, J. Hrubec, M. Jeitler¹, W. Kiesenhofer, V. Knünz, M. Krammer¹, I. Krätschmer, D. Liko, I. Mikulec, D. Rabady², B. Rahbaran, H. Rohringer, R. Schöfbeck, J. Strauss, A. Taurok, W. Treberer-Treberspurg, W. Waltenberger, C.-E. Wulz¹

National Centre for Particle and High Energy Physics, Minsk, Belarus

V. Mossolov, N. Shumeiko, J. Suarez Gonzalez

Universiteit Antwerpen, Antwerp, Belgium

S. Alderweireldt, M. Bansal, S. Bansal, T. Cornelis, E. A. De Wolf, X. Janssen, A. Knutsson, S. Luyckx, L. Mucibello, S. Ochesanu, B. Roland, R. Rougny, H. Van Haevermaet, P. Van Mechelen, N. Van Remortel, A. Van Spilbeeck

Vrije Universiteit Brussel, Brussels, Belgium

F. Blekman, S. Blyweert, J. D'Hondt, N. Heracleous, A. Kalogeropoulos, J. Keaveney, T. J. Kim, S. Lowette, M. Maes, A. Olbrechts, D. Strom, S. Tavernier, W. Van Doninck, P. Van Mulders, G. P. Van Onsem, I. Villella

Université Libre de Bruxelles, Brussels, Belgium

C. Caillol, B. Clerbaux, G. De Lentdecker, L. Favart, A. P. R. Gay, A. Léonard, P. E. Marage, A. Mohammadi, L. Perniè, T. Reis, T. Seva, L. Thomas, C. Vander Velde, P. Vanlaer, J. Wang

Ghent University, Ghent, Belgium

V. Adler, K. Beernaert, L. Benucci, A. Cimmino, S. Costantini, S. Dildick, G. Garcia, B. Klein, J. Lellouch, J. McCartin, A. A. Ocampo Rios, D. Ryckbosch, S. Salva Diblen, M. Sigamani, N. Strobbe, F. Thyssen, M. Tytgat, S. Walsh, E. Yazgan, N. Zaganidis

Université Catholique de Louvain, Louvain-la-Neuve, Belgium

S. Basegmez, C. Beluffi³, G. Bruno, R. Castello, A. Caudron, L. Ceard, G. G. Da Silveira, C. Delaere, T. du Pree, D. Favart, L. Forthomme, A. Giammanco⁴, J. Hollar, P. Jez, M. Komm, V. Lemaitre, J. Liao, O. Militaru, C. Nuttens, D. Pagano, A. Pin, K. Piotrkowski, A. Popov⁵, L. Quertenmont, M. Selvaggi, M. Vidal Marono, J. M. Vizan Garcia

Université de Mons, Mons, Belgium

N. Bely, T. Caebergs, E. Daubie, G. H. Hammad

Centro Brasileiro de Pesquisas Fisicas, Rio de Janeiro, Brazil

G. A. Alves, M. Correa Martins Junior, T. Dos Reis Martins, M. E. Pol, M. H. G. Souza

Universidade do Estado do Rio de Janeiro, Rio de Janeiro, Brazil

W. L. Aldá Júnior, W. Carvalho, J. Chinellato⁶, A. Custódio, E. M. Da Costa, D. De Jesus Damiao, C. De Oliveira Martins, S. Fonseca De Souza, H. Malbouisson, M. Malek, D. Matos Figueiredo, L. Mundim, H. Nogima, W. L. Prado Da Silva, J. Santaolalla, A. Santoro, A. Sznajder, E. J. Tonelli Manganote⁶, A. Vilela Pereira

Universidade Estadual Paulista^a, Universidade Federal do ABC^b, São Paulo, Brazil

C. A. Bernardes^b, F. A. Dias^{a,7}, T. R. Fernandez Perez Tomei^a, E. M. Gregores^b, P. G. Mercadante^b, S. F. Novaes^a, Sandra S. Padula^a

Institute for Nuclear Research and Nuclear Energy, Sofia, Bulgaria

V. Genchev², P. Iaydjiev², A. Marinov, S. Piperov, M. Rodozov, G. Sultanov, M. Vutova

University of Sofia, Sofia, Bulgaria

A. Dimitrov, I. Glushkov, R. Hadjiiska, V. Kozuharov, L. Litov, B. Pavlov, P. Petkov

Institute of High Energy Physics, Beijing, China

J. G. Bian, G. M. Chen, H. S. Chen, M. Chen, R. Du, C. H. Jiang, D. Liang, S. Liang, X. Meng, R. Plestina⁸, J. Tao, X. Wang, Z. Wang

State Key Laboratory of Nuclear Physics and Technology, Peking University, Beijing, China

C. Asawatangtrakuldee, Y. Ban, Y. Guo, Q. Li, W. Li, S. Liu, Y. Mao, S. J. Qian, D. Wang, L. Zhang, W. Zou

Universidad de Los Andes, Bogota, Colombia

C. Avila, C. A. Carrillo Montoya, L. F. Chaparro Sierra, C. Florez, J. P. Gomez, B. Gomez Moreno, J. C. Sanabria

Technical University of Split, Split, Croatia

N. Godinovic, D. Lelas, D. Polic, I. Puljak

University of Split, Split, Croatia

Z. Antunovic, M. Kovac

Institute Rudjer Boskovic, Zagreb, Croatia

V. Brigljevic, K. Kadija, J. Luetic, D. Mekterovic, S. Morovic, L. Sudic

University of Cyprus, Nicosia, Cyprus

A. Attikis, G. Mavromanolakis, J. Mousa, C. Nicolaou, F. Ptochos, P. A. Razis

Charles University, Prague, Czech Republic

M. Finger, M. Finger Jr.

Academy of Scientific Research and Technology of the Arab Republic of Egypt, Egyptian Network of High Energy Physics, Cairo, Egypt

A. A. Abdelalim⁹, Y. Assran¹⁰, S. Elgammal¹¹, A. Ellithi Kamel¹², M. A. Mahmoud¹³, A. Radi^{11,14}

National Institute of Chemical Physics and Biophysics, Tallinn, Estonia

M. Kadastik, M. Müntel, M. Murumaa, M. Raidal, L. Rebane, A. Tiko

Department of Physics, University of Helsinki, Helsinki, Finland

P. Eerola, G. Fedi, M. Voutilainen

Helsinki Institute of Physics, Helsinki, Finland

J. Härkönen, V. Karimäki, R. Kinnunen, M. J. Kortelainen, T. Lampén, K. Lassila-Perini, S. Lehti, T. Lindén, P. Luukka, T. Mäenpää, T. Peltola, E. Tuominen, J. Tuominiemi, E. Tuovinen, L. Wendland

Lappeenranta University of Technology, Lappeenranta, Finland

T. Tuuva

DSM/IRFU, CEA/Saclay, Gif-sur-Yvette, France

M. Besancon, F. Couderc, M. Dejarin, D. Denegri, B. Fabbro, J. L. Faure, F. Ferri, S. Ganjour, A. Givernaud, P. Gras, G. Hamel de Monchenault, P. Jarry, E. Locci, J. Malcles, A. Nayak, J. Rander, A. Rosowsky, M. Titov

Laboratoire Leprince-Ringuet, Ecole Polytechnique, IN2P3-CNRS, Palaiseau, France

S. Baffioni, F. Beaudette, P. Busson, C. Charlot, N. Daci, T. Dahms, M. Dalchenko, L. Dobrzynski, A. Florent, R. Granier de Cassagnac, P. Miné, C. Mironov, I. N. Naranjo, M. Nguyen, C. Ochando, P. Paganini, D. Sabes, R. Salerno, J. B. Sauvan, Y. Sirois, C. Veelken, Y. Yilmaz, A. Zabi

Institut Pluridisciplinaire Hubert Curien, Université de Strasbourg, Université de Haute Alsace Mulhouse, CNRS/IN2P3, Strasbourg, France

J.-L. Agram¹⁵, J. Andrea, D. Bloch, J.-M. Brom, E. C. Chabert, C. Collard, E. Conte¹⁵, F. Drouhin¹⁵, J.-C. Fontaine¹⁵, D. Gelé, U. Goerlach, C. Goetzmann, P. Juillot, A.-C. Le Bihan, P. Van Hove

Centre de Calcul de l'Institut National de Physique Nucleaire et de Physique des Particules, CNRS/IN2P3, Villeurbanne, France

S. Gadrat

Institut de Physique Nucléaire de Lyon, Université de Lyon, Université Claude Bernard Lyon 1, CNRS-IN2P3, Villeurbanne, France

S. Beauceron, N. Beaupere, G. Boudoul, S. Brochet, J. Chasserat, R. Chierici, D. Contardo², P. Depasse, H. El Mamouni, J. Fan, J. Fay, S. Gascon, M. Gouzevitch, B. Ille, T. Kurca, M. Lethuillier, L. Mirabito, S. Perries, J. D. Ruiz Alvarez, L. Sgandurra, V. Sordini, M. Vander Donckt, P. Verdier, S. Viret, H. Xiao

Institute of High Energy Physics and Informatization, Tbilisi State University, Tbilisi, Georgia

Z. Tsamalaidze¹⁶

RWTH Aachen University, I. Physikalisches Institut, Aachen, Germany

C. Autermann, S. Beranek, M. Bontenackels, B. Calpas, M. Edelhoff, L. Feld, O. Hindrichs, K. Klein, A. Ostapchuk, A. Perieanu, F. Raupach, J. Sammet, S. Schael, D. Sprenger, H. Weber, B. Wittmer, V. Zhukov⁵

RWTH Aachen University, III. Physikalisches Institut A, Aachen, Germany

M. Ata, J. Caudron, E. Dietz-Laursonn, D. Duchardt, M. Erdmann, R. Fischer, A. Güth, T. Hebbeker, C. Heidemann, K. Hoepfner, D. Klingebiel, S. Knutzen, P. Kreuzer, M. Merschmeyer, A. Meyer, M. Olschewski, K. Padeken, P. Papacz, H. Reithler, S. A. Schmitz, L. Sonnenschein, D. Teyssier, S. Thüer, M. Weber

RWTH Aachen University, III. Physikalisches Institut B, Aachen, Germany

V. Cherepanov, Y. Erdogan, G. Flügge, H. Geenen, M. Geisler, W. Haj Ahmad, F. Hoehle, B. Kargoll, T. Kress, Y. Kuessel, J. Lingemann², A. Nowack, I. M. Nugent, L. Perchalla, O. Pooth, A. Stahl

Deutsches Elektronen-Synchrotron, Hamburg, Germany

I. Asin, N. Bartosik, J. Behr, W. Behrenhoff, U. Behrens, A. J. Bell, M. Bergholz¹⁷, A. Bethani, K. Borrás, A. Burgmeier, A. Cakir, L. Calligaris, A. Campbell, S. Choudhury, F. Costanza, C. Diez Pardos, S. Dooling, T. Dorland, G. Eckerlin, D. Eckstein, T. Eichhorn, G. Flucke, A. Geiser, A. Grebenyuk, P. Gunnellini, S. Habib, J. Hauk, G. Hellwig, M. Hempel, D. Horton, H. Jung, M. Kasemann, P. Katsas, J. Kieseler, C. Kleinwort, M. Krämer, D. Krücker, W. Lange, J. Leonard, K. Lipka, W. Lohmann¹⁷, B. Lutz, R. Mankel, I. Marfin, I.-A. Melzer-Pellmann, A. B. Meyer, J. Mnich, A. Mussgiller, S. Naumann-Emme, O. Novgorodova, F. Nowak, H. Perrey, A. Petrukhin, D. Pitzl, R. Placakyte, A. Raspereza, P. M. Ribeiro Cipriano, C. Riedl, E. Ron, M. Ö. Sahin, J. Salfeld-Nebgen, P. Saxena, R. Schmidt¹⁷, T. Schoerner-Sadenius, M. Schröder, M. Stein, A. D. R. Vargas Trevino, R. Walsh, C. Wissing

University of Hamburg, Hamburg, Germany

M. Aldaya Martin, V. Blobel, H. Enderle, J. Erfle, E. Garutti, K. Goebel, M. Görner, M. Gosselink, J. Haller, R. S. Höing, H. Kirschenmann, R. Klanner, R. Kogler, J. Lange, T. Lapsien, T. Lenz, I. Marchesini, J. Ott, T. Peiffer, N. Pietsch, D. Rathjens, C. Sander, H. Schettler, P. Schleper, E. Schlieckau, A. Schmidt, M. Seidel, J. Sibille¹⁸, V. Sola, H. Stadie, G. Steinbrück, D. Troendle, E. Usai, L. Vanelderen

Institut für Experimentelle Kernphysik, Karlsruhe, Germany

C. Barth, C. Baus, J. Berger, C. Böser, E. Butz, T. Chwalek, W. De Boer, A. Descroix, A. Dierlamm, M. Feindt, M. Guthoff², F. Hartmann², T. Hauth², H. Held, K. H. Hoffmann, U. Husemann, I. Katkov⁵, A. Kornmayer², E. Kuznetsova, P. Lobelle Pardo, D. Martschei, M. U. Mozer, Th. Müller, M. Niegel, A. Nürnberg, O. Oberst, G. Quast, K. Rabbertz, F. Ratnikov, S. Röcker, F.-P. Schilling, G. Schott, H. J. Simonis, F. M. Stober, R. Ulrich, J. Wagner-Kuhr, S. Wayand, T. Weiler, R. Wolf, M. Zeise

Institute of Nuclear and Particle Physics (INPP), NCSR Demokritos, Aghia Paraskevi, Greece

G. Anagnostou, G. Daskalakis, T. Geralis, S. Kesisoglou, A. Kyriakis, D. Loukas, A. Markou, C. Markou, E. Ntomari, A. Psallidas, I. Topsis-Giotis

University of Athens, Athens, Greece

L. Gouskos, A. Panagiotou, N. Saoulidou, E. Stiliaris

University of Ioánnina, Ioannina, Greece

X. Aslanoglou, I. Evangelou, G. Flouris, C. Foudas, J. Jones, P. Kokkas, N. Manthos, I. Papadopoulos, E. Paradas

Wigner Research Centre for Physics, Budapest, Hungary

G. Bencze, C. Hajdu, P. Hidas, D. Horvath¹⁹, F. Sikler, V. Veszpremi, G. Vesztergombi²⁰, A. J. Zsigmond

Institute of Nuclear Research ATOMKI, Debrecen, Hungary

N. Beni, S. Czellar, J. Molnar, J. Palinkas, Z. Szillasi

University of Debrecen, Debrecen, Hungary

J. Karacsi, P. Raics, Z. L. Trocsanyi, B. Ujvari

National Institute of Science Education and Research, Bhubaneswar, India

S. K. Swain

Panjab University, Chandigarh, India

S. B. Beri, V. Bhatnagar, N. Dhingra, R. Gupta, M. Kaur, M. Z. Mehta, M. Mittal, N. Nishu, A. Sharma, J. B. Singh

University of Delhi, Delhi, India

Ashok Kumar, Arun Kumar, S. Ahuja, A. Bhardwaj, B. C. Choudhary, A. Kumar, S. Malhotra, M. Naimuddin, K. Ranjan, V. Sharma, R. K. Shivpuri

Saha Institute of Nuclear Physics, Kolkata, India

S. Banerjee, S. Bhattacharya, K. Chatterjee, S. Dutta, B. Gomber, Sa. Jain, Sh. Jain, R. Khurana, A. Modak, S. Mukherjee, D. Roy, S. Sarkar, M. Sharan, A. P. Singh

Bhabha Atomic Research Centre, Mumbai, IndiaA. Abdulsalam, D. Dutta, S. Kailas, V. Kumar, A. K. Mohanty², L. M. Pant, P. Shukla, A. Topkar**Tata Institute of Fundamental Research-EHEP, Mumbai, India**T. Aziz, R. M. Chatterjee, S. Ganguly, S. Ghosh, M. Guchait²¹, A. Gurtu²², G. Kole, S. Kumar, M. Maity²³, G. Majumder, K. Mazumdar, G. B. Mohanty, B. Parida, K. Sudhakar, N. Wickramage²⁴**Tata Institute of Fundamental Research-HECR, Mumbai, India**

S. Banerjee, S. Dugad

Institute for Research in Fundamental Sciences (IPM), Tehran, IranH. Arfaei, H. Bakhshiansohi, H. Behnamian, S. M. Etesami²⁵, A. Fahim²⁶, A. Jafari, M. Khakzad, M. Mohammadi Najafabadi, M. Naseri, S. Paktinat Mehdiabadi, B. Safarzadeh²⁷, M. Zeinali**University College Dublin, Dublin, Ireland**

M. Grunewald

INFN Sezione di Bari^a, Università di Bari^b, Politecnico di Bari^c, Bari, ItalyM. Abbrescia^{a,b}, L. Barbore^{a,b}, C. Calabria^{a,b}, S. S. Chhibra^{a,b}, A. Colaleo^a, D. Creanza^{a,c}, N. De Filippis^{a,c}, M. De Palma^{a,b}, L. Fiore^a, G. Iaselli^{a,c}, G. Maggi^{a,c}, M. Maggi^a, B. Marangelli^{a,b}, S. My^{a,c}, S. Nuzzo^{a,b}, N. Pacifico^a, A. Pompili^{a,b}, G. Pugliese^{a,c}, R. Radogna^{a,b}, G. Selvaggi^{a,b}, L. Silvestris^a, G. Singh^{a,b}, R. Venditti^{a,b}, P. Verwilligen^a, G. Zito^a**INFN Sezione di Bologna^a, Università di Bologna^b, Bologna, Italy**G. Abbiendi^a, A. C. Benvenuti^a, D. Bonacorsi^{a,b}, S. Braibant-Giacomelli^{a,b}, L. Brigliadori^{a,b}, R. Campanini^{a,b}, P. Capiluppi^{a,b}, A. Castro^{a,b}, F. R. Cavallo^a, G. Codispoti^{a,b}, M. Cuffiani^{a,b}, G. M. Dallavalle^a, F. Fabbri^a, A. Fanfani^{a,b}, D. Fasanella^{a,b}, P. Giacomelli^a, C. Grandi^a, L. Guiducci^{a,b}, S. Marcellini^a, G. Masetti^a, M. Meneghelli^{a,b}, A. Montanari^a, F. L. Navarria^{a,b}, F. Odoricci^a, A. Perrotta^a, F. Primavera^{a,b}, A. M. Rossi^{a,b}, T. Rovelli^{a,b}, G. P. Siroli^{a,b}, N. Tosi^{a,b}, R. Travaglini^{a,b}**INFN Sezione di Catania^a, Università di Catania^b, CSFNSM^c, Catania, Italy**S. Albergo^{a,b}, G. Cappello^a, M. Chiorboli^{a,b}, S. Costa^{a,b}, F. Giordano^{a,2}, R. Potenza^{a,b}, A. Tricomi^{a,b}, C. Tuve^{a,b}**INFN Sezione di Firenze^a, Università di Firenze^b, Florence, Italy**G. Barbagli^a, V. Ciulli^{a,b}, C. Civinini^a, R. D'Alessandro^{a,b}, E. Focardi^{a,b}, E. Gallo^a, S. Gonzi^{a,b}, V. Gori^{a,b}, P. Lenzi^{a,b}, M. Meschini^a, S. Paoletti^a, G. Sguazzoni^a, A. Tropiano^{a,b}**INFN Laboratori Nazionali di Frascati, Frascati, Italy**

L. Benussi, S. Bianco, F. Fabbri, D. Piccolo

INFN Sezione di Genova^a, Università di Genova^b, Genoa, ItalyP. Fabbriatore^a, R. Ferretti^{a,b}, F. Ferro^a, M. Lo Vetere^{a,b}, R. Musenich^a, E. Robutti^a, S. Tosi^{a,b}**INFN Sezione di Milano-Bicocca^a, Università di Milano-Bicocca^b, Milan, Italy**A. Benaglia^a, M. E. Dinardo^{a,b}, S. Fiorendi^{a,b,2}, S. Gennai^a, R. Gerosa, A. Ghezzi^{a,b}, P. Govoni^{a,b}, M. T. Lucchini^{a,b,2}, S. Malvezzi^a, R. A. Manzoni^{a,b,2}, A. Martelli^{a,b,2}, B. Marzocchi, D. Menasce^a, L. Moroni^a, M. Paganoni^{a,b}, D. Pedrini^a, S. Ragazzi^{a,b}, N. Redaelli^a, T. Tabarelli de Fatis^{a,b}**INFN Sezione di Napoli^a, Università di Napoli 'Federico II'^b, Università della Basilicata (Potenza)^c, Università G. Marconi (Roma)^d, Naples, Italy**S. Buontempo^a, N. Cavallo^{a,c}, F. Fabozzi^{a,c}, A. O. M. Iorio^{a,b}, L. Lista^a, S. Meola^{a,d,2}, M. Merola^a, P. Paolucci^{a,2}**INFN Sezione di Padova^a, Università di Padova^b, Università di Trento (Trento)^c, Padua, Italy**P. Azzi^a, N. Bacchetta^a, A. Branca^{a,b}, R. Carlin^{a,b}, P. Checchia^a, T. Dorigo^a, U. Dosselli^a, M. Galanti^{a,b,2}, F. Gasparini^{a,b}, U. Gasparini^{a,b}, P. Giubilato^{a,b}, A. Gozzelino^a, K. Kanishev^{a,c}, S. Lacaprara^a, I. Lazzizzera^{a,c}, M. Margoni^{a,b}, A. T. Meneguzzo^{a,b}, J. Pazzini^{a,b}, M. Pegoraro^a, N. Pozzobon^{a,b}, P. Ronchese^{a,b}, F. Simonetto^{a,b}, E. Torassa^a, M. Tosi^{a,b}, A. Triossi^a, S. Ventura^a, P. Zotto^{a,b}, A. Zucchetta^{a,b}, G. Zumerle^{a,b}**INFN Sezione di Pavia^a, Università di Pavia^b, Pavia, Italy**M. Gabusi^{a,b}, S. P. Ratti^{a,b}, C. Riccardi^{a,b}, P. Vitulo^{a,b}

INFN Sezione di Perugia^a, Università di Perugia^b, Perugia, Italy

M. Biasini^{a,b}, G. M. Bilei^a, L. Fanò^{a,b}, P. Lariccia^{a,b}, G. Mantovani^{a,b}, M. Menichelli^a, F. Romeo^{a,b}, A. Saha^a, A. Santocchia^{a,b}, A. Spiezia^{a,b}

INFN Sezione di Pisa^a, Università di Pisa^b, Scuola Normale Superiore di Pisa^c, Pisa, Italy

K. Androsova^{a,28}, P. Azzurri^a, G. Bagliesi^a, J. Bernardini^a, T. Boccali^a, G. Broccolo^{a,c}, R. Castaldi^a, M. A. Ciocci^{a,28}, R. Dell'Orso^a, F. Fiori^{a,c}, L. Foà^{a,c}, A. Giassi^a, M. T. Grippo^{a,28}, A. Kraan^a, F. Ligabue^{a,c}, T. Lomtadze^a, L. Martini^{a,b}, A. Messineo^{a,b}, C. S. Moon^{a,29}, F. Palla^a, A. Rizzi^{a,b}, A. Savoy-Navarro^{a,30}, A. T. Serban^a, P. Spagnolo^a, P. Squillacioti^{a,28}, R. Tenchini^a, G. Tonelli^{a,b}, A. Venturi^a, P. G. Verdini^a, C. Vernieri^{a,c}

INFN Sezione di Roma^a, Università di Roma^b, Rome, Italy

L. Barone^{a,b}, F. Cavallari^a, D. Del Re^{a,b}, M. Diemoz^a, M. Grassi^{a,b}, C. Jorda^a, E. Longo^{a,b}, F. Margaroli^{a,b}, P. Meridiani^a, F. Micheli^{a,b}, S. Nourbakhsh^{a,b}, G. Organtini^{a,b}, R. Paramatti^a, S. Rahatlou^{a,b}, C. Rovelli^a, L. Soffi^{a,b}, P. Traczyk^{a,b}

INFN Sezione di Torino^a, Università di Torino^b, Università del Piemonte Orientale (Novara)^c, Turin, Italy

N. Amapane^{a,b}, R. Arcidiacono^{a,c}, S. Argiro^{a,b}, M. Arneodo^{a,c}, R. Bellan^{a,b}, C. Biino^a, N. Cartiglia^a, S. Casasso^{a,b}, M. Costa^{a,b}, A. Degano^{a,b}, N. Demaria^a, C. Mariotti^a, S. Maselli^a, E. Migliore^{a,b}, V. Monaco^{a,b}, M. Musich^a, M. M. Obertino^{a,c}, G. Ortona^{a,b}, L. Pacher^{a,b}, N. Pastrone^a, M. Pelliccioni^{a,2}, A. Potenza^{a,b}, A. Romero^{a,b}, M. Ruspai^{a,c}, R. Sacchi^{a,b}, A. Solano^{a,b}, A. Staiano^a, U. Tamponi^a

INFN Sezione di Trieste^a, Università di Trieste^b, Trieste, Italy

S. Belforte^a, V. Candelise^{a,b}, M. Casarsa^a, F. Cossutti^a, G. Della Ricca^{a,b}, B. Gobbo^a, C. La Licata^{a,b}, M. Marone^{a,b}, D. Montanino^{a,b}, A. Penzo^a, A. Schizzi^{a,b}, T. Umer^{a,b}, A. Zanetti^a

Kangwon National University, Chuncheon, Korea

S. Chang, T. Y. Kim, S. K. Nam

Kyungpook National University, Taegu, Korea

D. H. Kim, G. N. Kim, J. E. Kim, M. S. Kim, D. J. Kong, S. Lee, Y. D. Oh, H. Park, D. C. Son

Institute for Universe and Elementary Particles, Chonnam National University, Kwangju, Korea

J. Y. Kim, Zero J. Kim, S. Song

Korea University, Seoul, Korea

S. Choi, D. Gyun, B. Hong, M. Jo, H. Kim, Y. Kim, K. S. Lee, S. K. Park, Y. Roh

University of Seoul, Seoul, Korea

M. Choi, J. H. Kim, C. Park, I. C. Park, S. Park, G. Ryu

Sungkyunkwan University, Suwon, Korea

Y. Choi, Y. K. Choi, J. Goh, E. Kwon, B. Lee, J. Lee, H. Seo, I. Yu

Vilnius University, Vilnius, Lithuania

A. Juodagalvis

National Centre for Particle Physics, Universiti Malaya, Kuala Lumpur, Malaysia

J. R. Komaragiri

Centro de Investigacion y de Estudios Avanzados del IPN, Mexico City, Mexico

H. Castilla-Valdez, E. De La Cruz-Burelo, I. Heredia-de La Cruz³¹, R. Lopez-Fernandez, J. Martínez-Ortega, A. Sanchez-Hernandez, L. M. Villasenor-Cendejas

Universidad Iberoamericana, Mexico City, Mexico

S. Carrillo Moreno, F. Vazquez Valencia

Benemerita Universidad Autonoma de Puebla, Puebla, Mexico

H. A. Salazar Ibarquen

Universidad Autónoma de San Luis Potosí, San Luis Potosí, Mexico

E. Casimiro Linares, A. Morelos Pineda

University of Auckland, Auckland, New Zealand

D. Krofcheck

University of Canterbury, Christchurch, New Zealand

P. H. Butler, R. Doesburg, S. Reucroft

National Centre for Physics, Quaid-I-Azam University, Islamabad, Pakistan

M. Ahmad, M. I. Asghar, J. Butt, H. R. Hoorani, W. A. Khan, T. Khurshid, S. Qazi, M. A. Shah, M. Shoaib

National Centre for Nuclear Research, Swierk, PolandH. Bialkowska, M. Bluj³², B. Boimska, T. Frueboes, M. Górski, M. Kazana, K. Nawrocki, K. Romanowska-Rybinska, M. Szleper, G. Wrochna, P. Zalewski**Faculty of Physics, Institute of Experimental Physics, University of Warsaw, Warsaw, Poland**

G. Brona, K. Bunkowski, M. Cwiok, W. Dominik, K. Doroba, A. Kalinowski, M. Konecki, J. Krolikowski, M. Misiura, W. Wolszczak

Laboratório de Instrumentação e Física Experimental de Partículas, Lisbon, PortugalP. Bargassa, C. Beirão Da Cruz E Silva, P. Faccioli, P. G. Ferreira Parracho, M. Gallinaro, F. Nguyen, J. Rodrigues Antunes, J. Seixas², J. Varela, P. Vischia**Joint Institute for Nuclear Research, Dubna, Russia**S. Afanasiev, P. Bunin, I. Golutvin, I. Gorbunov, A. Kamenev, V. Karjavin, V. Konoplyanikov, G. Kozlov, A. Lanev, A. Malakhov, V. Matveev³³, P. Moisezenz, V. Palichik, V. Perelygin, S. Shmatov, N. Skatchkov, V. Smirnov, A. Zarubin**Petersburg Nuclear Physics Institute, Gatchina (St. Petersburg), Russia**V. Golovtsov, Y. Ivanov, V. Kim³⁴, P. Levchenko, V. Murzin, V. Oreshkin, I. Smirnov, V. Sulimov, L. Uvarov, S. Vavilov, A. Vorobyev, An. Vorobyev**Institute for Nuclear Research, Moscow, Russia**

Yu. Andreev, A. Dermenev, S. Gninenko, N. Golubev, M. Kirsanov, N. Krasnikov, A. Pashenkov, D. Tlisov, A. Toropin

Institute for Theoretical and Experimental Physics, Moscow, Russia

V. Epshteyn, V. Gavrilov, N. Lychkovskaya, V. Popov, G. Safronov, S. Semenov, A. Spiridonov, V. Stolin, E. Vlasov, A. Zhokin

P.N. Lebedev Physical Institute, Moscow, Russia

V. Andreev, M. Azarkin, I. Dremin, M. Kirakosyan, A. Leonidov, G. Mesyats, S. V. Rusakov, A. Vinogradov

Skobeltsyn Institute of Nuclear Physics, Lomonosov Moscow State University, Moscow, Russia

A. Belyaev, G. Bogdanova, E. Boos, L. Khein, V. Klyukhin, O. Kodolova, I. Lokhtin, O. Lukina, S. Obraztsov, S. Petrushanko, A. Proskuryakov, V. Savrin, V. Volkov

State Research Center of Russian Federation, Institute for High Energy Physics, Protvino, Russia

I. Azhgirey, I. Bayshev, S. Bitiukov, V. Kachanov, A. Kalinin, D. Konstantinov, V. Krychkine, V. Petrov, R. Ryutin, A. Sobol, L. Tourtchanovitch, S. Troshin, N. Tyurin, A. Uzunian, A. Volkov

Faculty of Physics and Vinca Institute of Nuclear Sciences, University of Belgrade, Belgrade, SerbiaP. Adzic³⁵, M. Dordevic, M. Ekmedzic, J. Milosevic**Centro de Investigaciones Energéticas Medioambientales y Tecnológicas (CIEMAT), Madrid, Spain**M. Aguilar-Benitez, J. Alcaraz Maestre, C. Battilana, E. Calvo, M. Cerrada, M. Chamizo Llatas², N. Colino, B. De La Cruz, A. Delgado Peris, D. Domínguez Vázquez, C. Fernandez Bedoya, J. P. Fernández Ramos, A. Ferrando, J. Flix, M. C. Fouz, P. Garcia-Abia, O. Gonzalez Lopez, S. Goy Lopez, J. M. Hernandez, M. I. Josa, G. Merino, E. Navarro De Martino, J. Puerta Pelayo, A. Quintario Olmeda, I. Redondo, L. Romero, M. S. Soares, C. Willmott**Universidad Autónoma de Madrid, Madrid, Spain**

C. Albajar, J. F. de Trocóniz, M. Missiroli

Universidad de Oviedo, Oviedo, Spain

H. Brun, J. Cuevas, J. Fernandez Menendez, S. Folgueras, I. Gonzalez Caballero, L. Lloret Iglesias

Instituto de Física de Cantabria (IFCA), CSIC-Universidad de Cantabria, Santander, Spain

J. A. Brochero Cifuentes, I. J. Cabrillo, A. Calderon, J. Duarte Campderros, M. Fernandez, G. Gomez, J. Gonzalez Sanchez, A. Graziano, A. Lopez Virto, J. Marco, R. Marco, C. Martinez Rivero, F. Matorras, F. J. Munoz Sanchez, J. Piedra Gomez, T. Rodrigo, A. Y. Rodríguez-Marrero, A. Ruiz-Jimeno, L. Scodellaro, I. Vila, R. Vilar Cortabitarte

CERN, European Organization for Nuclear Research, Geneva, Switzerland

D. Abbaneo, E. Auffray, G. Auzinger, M. Bachtis, P. Baillon, A. H. Ball, D. Barney, J. Bendavid, L. Benhabib, J. F. Benitez, C. Bernet⁸, G. Bianchi, P. Bloch, A. Bocci, A. Bonato, O. Bondu, C. Botta, H. Breuker, T. Camporesi, G. Cerminara, T. Christiansen, J. A. Coarasa Perez, S. Colafranceschi³⁶, M. D'Alfonso, D. d'Enterria, A. Dabrowski, A. David, F. De Guio, A. De Roeck, S. De Visscher, S. Di Guida, M. Dobson, N. Dupont-Sagorin, A. Elliott-Peisert, J. Eugster, G. Franzoni, W. Funk, M. Giffels, D. Gigi, K. Gill, D. Giordano, M. Girone, M. Giunta, F. Glege, R. Gomez-Reino Garrido, S. Gowdy, R. Guida, J. Hammer, M. Hansen, P. Harris, V. Innocente, P. Janot, E. Karavakis, K. Kousouris, K. Krajczar, P. Lecoq, C. Lourenço, N. Magini, L. Malgeri, M. Mannelli, L. Masetti, F. Meijers, S. Mersi, E. Meschi, F. Moortgat, M. Mulders, P. Musella, L. Orsini, E. Palencia Cortezon, E. Perez, L. Perrozzi, A. Petrilli, G. Petrucciani, A. Pfeiffer, M. Pierini, M. Pimiä, D. Piparo, M. Plagge, A. Racz, W. Reece, G. Rolandi³⁷, M. Rovere, H. Sakulin, F. Santanastasio, C. Schäfer, C. Schwick, S. Sekmen, A. Sharma, P. Siegrist, P. Silva, M. Simon, P. Sphicas³⁸, D. Spiga, J. Steggemann, B. Stieger, M. Stoye, A. Tsiros, G. I. Veres²⁰, J. R. Vlimant, H. K. Wöhri, W. D. Zeuner

Paul Scherrer Institut, Villigen, Switzerland

W. Bertl, K. Deiters, W. Erdmann, R. Horisberger, Q. Ingram, H. C. Kaestli, S. König, D. Kotlinski, U. Langenegger, D. Renker, T. Rohe

Institute for Particle Physics, ETH Zurich, Zurich, Switzerland

F. Bachmair, L. Bäni, L. Bianchini, P. Bortignon, M. A. Buchmann, B. Casal, N. Chanon, A. Deisher, G. Dissertori, M. Dittmar, M. Donegà, M. Dünser, P. Eller, C. Grab, D. Hits, W. Luster, B. Mangano, A. C. Marini, P. Martinez Ruiz del Arbol, D. Meister, N. Mohr, C. Nageli³⁹, P. Nef, F. Nessi-Tedaldi, F. Pandolfi, L. Pape, F. Pauss, M. Peruzzi, M. Quitnat, F. J. Ronga, M. Rossini, A. Starodumov⁴⁰, M. Takahashi, L. Tauscher[†], K. Theofilatos, D. Treille, R. Wallny, H. A. Weber

Universität Zürich, Zurich, Switzerland

C. AMSLER⁴¹, V. Chiochia, A. De Cosa, C. Favaro, A. Hinzmann, T. Hreus, M. Ivova Rikova, B. Kilminster, B. Millan Mejias, J. Ngadiuba, P. Robmann, H. Snoek, S. Taroni, M. Verzetti, Y. Yang

National Central University, Chung-Li, Taiwan

M. Cardaci, K. H. Chen, C. Ferro, C. M. Kuo, S. W. Li, W. Lin, Y. J. Lu, R. Volpe, S. S. Yu

National Taiwan University (NTU), Taipei, Taiwan

P. Bartalini, P. Chang, Y. H. Chang, Y. W. Chang, Y. Chao, K. F. Chen, P. H. Chen, C. Dietz, U. Grundler, W.-S. Hou, Y. Hsiung, K. Y. Kao, Y. J. Lei, Y. F. Liu, R.-S. Lu, D. Majumder, E. Petrakou, X. Shi, J. G. Shiu, Y. M. Tzeng, M. Wang, R. Wilken

Chulalongkorn University, Bangkok, Thailand

B. Asavapibhop, N. Suwonjandee

Cukurova University, Adana, Turkey

A. Adiguzel, M. N. Bakirci⁴², S. Cerci⁴³, C. Dozen, I. Dumanoglu, E. Eskut, S. Girgis, G. Gokbulut, E. Gurpinar, I. Hos, E. Kangal, A. Kayis Topaksu, G. Onengut⁴⁴, K. Ozdemir, S. Ozturk⁴², A. Polatoz, K. Sogut⁴⁵, D. Sunar Cerci⁴³, B. Tali⁴³, H. Topakli⁴², M. Vergili

Physics Department, Middle East Technical University, Ankara, Turkey

I. V. Akin, T. Aliev, B. Bilin, S. Bilmis, M. Deniz, H. Gamsizkan, A. M. Guler, G. Karapinar⁴⁶, K. Ocalan, A. Ozpineci, M. Serin, R. Sever, U. E. Surat, M. Yalvac, M. Zeyrek

Bogazici University, Istanbul, Turkey

E. Gülmez, B. Isildak⁴⁷, M. Kaya⁴⁸, O. Kaya⁴⁸, S. Ozkorucuklu⁴⁹

Istanbul Technical University, Istanbul, Turkey

H. Bahtiyar⁵⁰, E. Barlas, K. Cankocak, Y. O. Günaydin⁵¹, F. I. Vardarli, M. Yücel

National Scientific Center, Kharkov Institute of Physics and Technology, Kharkiv, Ukraine

L. Levchuk, P. Sorokin

University of Bristol, Bristol, UK

J. J. Brooke, E. Clement, D. Cussans, H. Flacher, R. Frazier, J. Goldstein, M. Grimes, G. P. Heath, H. F. Heath, J. Jacob, L. Kreczko, C. Lucas, Z. Meng, D. M. Newbold⁵², S. Paramesvaran, A. Poll, S. Senkin, V. J. Smith, T. Williams

Rutherford Appleton Laboratory, Didcot, UK

K. W. Bell, A. Belyaev⁵³, C. Brew, R. M. Brown, D. J. A. Cockerill, J. A. Coughlan, K. Harder, S. Harper, J. Ilic, E. Olaiya, D. Petyt, C. H. Shepherd-Themistocleous, A. Thea, I. R. Tomalin, W. J. Womersley, S. D. Worm

Imperial College, London, UK

M. Baber, R. Bainbridge, O. Buchmuller, D. Burton, D. Colling, N. Cripps, M. Cutajar, P. Dauncey, G. Davies, M. Della Negra, W. Ferguson, J. Fulcher, D. Futyan, A. Gilbert, A. Guneratne Bryer, G. Hall, Z. Hatherell, J. Hays, G. Iles, M. Jarvis, G. Karapostoli, M. Kenzie, R. Lane, R. Lucas⁵², L. Lyons, A.-M. Magnan, J. Marrouche, B. Mathias, R. Nandi, J. Nash, A. Nikitenko⁴⁰, J. Pela, M. Pesaresi, K. Petridis, M. Pioppi⁵⁴, D. M. Raymond, S. Rogerson, A. Rose, C. Seez, P. Sharp[†], A. Sparrow, A. Tapper, M. Vazquez Acosta, T. Virdee, S. Wakefield, N. Wardle

Brunel University, Uxbridge, UK

J. E. Cole, P. R. Hobson, A. Khan, P. Kyberd, D. Leggat, D. Leslie, W. Martin, I. D. Reid, P. Symonds, L. Teodorescu, M. Turner

Baylor University, Waco, USA

J. Dittmann, K. Hatakeyama, A. Kasmi, H. Liu, T. Scarborough

The University of Alabama, Tuscaloosa, USA

O. Charaf, S. I. Cooper, C. Henderson, P. Rumerio

Boston University, Boston, USA

A. Avetisyan, T. Bose, C. Fantasia, A. Heister, P. Lawson, D. Lazic, J. Rohlf, D. Sperka, J. St. John, L. Sulak

Brown University, Providence, USA

J. Alimena, S. Bhattacharya, G. Christopher, D. Cutts, Z. Demiragli, A. Ferapontov, A. Garabedian, U. Heintz, S. Jabeen, G. Kukartsev, E. Laird, G. Landsberg, M. Luk, M. Narain, M. Segala, T. Sinthuprasith, T. Speer, J. Swanson

University of California, Davis, Davis, USA

R. Breedon, G. Breto, M. Calderon De La Barca Sanchez, S. Chauhan, M. Chertok, J. Conway, R. Conway, P. T. Cox, R. Erbacher, M. Gardner, W. Ko, A. Kopecky, R. Lander, T. Miceli, D. Pellett, J. Pilot, F. Ricci-Tam, B. Rutherford, M. Searle, S. Shalhout, J. Smith, M. Squires, M. Tripathi, S. Wilbur, R. Yohay

University of California, Los Angeles, USA

V. Andreev, D. Cline, R. Cousins, S. Erhan, P. Everaerts, C. Farrell, M. Felcini, J. Hauser, M. Ignatenko, C. Jarvis, G. Rakness, P. Schlein[†], E. Takasugi, V. Valuev, M. Weber

University of California, Riverside, Riverside, USA

J. Babb, R. Clare, J. Ellison, J. W. Gary, G. Hanson, J. Heilman, P. Jandir, F. Lacroix, H. Liu, O. R. Long, A. Luthra, M. Malberti, H. Nguyen, A. Shrinivas, J. Sturdy, S. Sumowidagdo, S. Wimpenny

University of California, San Diego, La Jolla, USA

W. Andrews, J. G. Branson, G. B. Cerati, S. Cittolin, R. T. D'Agnolo, D. Evans, A. Holzner, R. Kelley, D. Kovalskyi, M. Lebourgeois, J. Letts, I. Macneill, S. Padhi, C. Palmer, M. Pieri, M. Sani, V. Sharma, S. Simon, E. Sudano, M. Tadel, Y. Tu, A. Vartak, S. Wasserbaech⁵⁵, F. Würthwein, A. Yagil, J. Yoo

University of California, Santa Barbara, Santa Barbara, USA

D. Barge, C. Campagnari, T. Danielson, K. Flowers, P. Geffert, C. George, F. Golf, J. Incandela, C. Justus, R. Magaña Villalba, N. Mccoll, V. Pavlunin, J. Richman, R. Rossin, D. Stuart, W. To, C. West

California Institute of Technology, Pasadena, USA

A. Apresyan, A. Bornheim, J. Bunn, Y. Chen, E. Di Marco, J. Duarte, D. Kcira, A. Mott, H. B. Newman, C. Pena, C. Rogan, M. Spiropulu, V. Timciuc, R. Wilkinson, S. Xie, R. Y. Zhu

Carnegie Mellon University, Pittsburgh, USA

V. Azzolini, A. Calamba, R. Carroll, T. Ferguson, Y. Iiyama, D. W. Jang, M. Paulini, J. Russ, H. Vogel, I. Vorobiev

University of Colorado at Boulder, Boulder, USA

J. P. Cumalat, B. R. Drell, W. T. Ford, A. Gaz, E. Luiggi Lopez, U. Nauenberg, J. G. Smith, K. Stenson, K. A. Ulmer, S. R. Wagner

Cornell University, Ithaca, USA

J. Alexander, A. Chatterjee, N. Eggert, L. K. Gibbons, W. Hopkins, A. Khukhunaishvili, B. Kreis, N. Mirman, G. Nicolas Kaufman, J. R. Patterson, A. Ryd, E. Salvati, W. Sun, W. D. Teo, J. Thom, J. Thompson, J. Tucker, Y. Weng, L. Winstrom, P. Wittich

Fairfield University, Fairfield, USA

D. Winn

Fermi National Accelerator Laboratory, Batavia, USA

S. Abdullin, M. Albrow, J. Anderson, G. Apollinari, L. A. T. Bauerdick, A. Beretvas, J. Berryhill, P. C. Bhat, K. Burkett, J. N. Butler, V. Chetluru, H. W. K. Cheung, F. Chlebana, S. Cihangir, V. D. Elvira, I. Fisk, J. Freeman, Y. Gao, E. Gottschalk, L. Gray, D. Green, S. Grünendahl, O. Gutsche, D. Hare, R. M. Harris, J. Hirschauer, B. Hooberman, S. Jindariani, M. Johnson, U. Joshi, K. Kaadze, B. Klima, S. Kwan, J. Linacre, D. Lincoln, R. Lipton, J. Lykken, K. Maeshima, J. M. Marraffino, V. I. Martinez Outschoorn, S. Maruyama, D. Mason, P. McBride, K. Mishra, S. Mrenna, Y. Musienko³³, S. Nahn, C. Newman-Holmes, V. O'Dell, O. Prokofyev, N. Ratnikova, E. Sexton-Kennedy, S. Sharma, W. J. Spalding, L. Spiegel, L. Taylor, S. Tkaczyk, N. V. Tran, L. Uplegger, E. W. Vaandering, R. Vidal, A. Whitbeck, J. Whitmore, W. Wu, F. Yang, J. C. Yun

University of Florida, Gainesville, USA

D. Acosta, P. Avery, D. Bourilkov, T. Cheng, S. Das, M. De Gruttola, G. P. Di Giovanni, D. Dobur, R. D. Field, M. Fisher, Y. Fu, I. K. Furic, J. Hugon, B. Kim, J. Konigsberg, A. Korytov, A. Kropivnitskaya, T. Kypreos, J. F. Low, K. Matchev, P. Milenovic⁵⁶, G. Mitselmakher, L. Muniz, A. Rinkevicius, L. Shchutska, N. Skhirtladze, M. Snowball, J. Yelton, M. Zakaria

Florida International University, Miami, USA

V. Gaultney, S. Hewamanage, S. Linn, P. Markowitz, G. Martinez, J. L. Rodriguez

Florida State University, Tallahassee, USA

T. Adams, A. Askew, J. Bochenek, J. Chen, B. Diamond, J. Haas, S. Hagopian, V. Hagopian, K. F. Johnson, H. Prosper, V. Veeraraghavan, M. Weinberg

Florida Institute of Technology, Melbourne, USA

M. M. Baarmand, B. Dorney, M. Hohlmann, H. Kalakhety, F. Yumiceva

University of Illinois at Chicago (UIC), Chicago, USA

M. R. Adams, L. Apanasevich, V. E. Bazterra, R. R. Betts, I. Bucinskaite, R. Cavanaugh, O. Evdokimov, L. Gauthier, C. E. Gerber, D. J. Hofman, S. Khalatyan, P. Kurt, D. H. Moon, C. O'Brien, C. Silkworth, P. Turner, N. Varelas

The University of Iowa, Iowa City, USA

U. Akgun, E. A. Albayrak⁵⁰, B. Bilki⁵⁷, W. Clarida, K. Dilsiz, F. Duru, M. Haytmyradov, J.-P. Merlo, H. Mermerkaya⁵⁸, A. Mestvirishvili, A. Moeller, J. Nachtman, H. Ogul, Y. Onel, F. Ozok⁵⁰, S. Sen, P. Tan, E. Tiras, J. Wetzel, T. Yetkin⁵⁹, K. Yi

Johns Hopkins University, Baltimore, USA

B. A. Barnett, B. Blumenfeld, S. Bolognesi, D. Fehling, A. V. Gritsan, P. Maksimovic, C. Martin, M. Swartz

The University of Kansas, Lawrence, USA

P. Baringer, A. Bean, G. Benelli, R. P. Kenny III, M. Murray, D. Noonan, S. Sanders, J. Sekaric, R. Stringer, Q. Wang, J. S. Wood

Kansas State University, Manhattan, USA

A. F. Barfuss, I. Chakaberia, A. Ivanov, S. Khalil, M. Makouski, Y. Maravin, L. K. Saini, S. Shrestha, I. Svintradze

Lawrence Livermore National Laboratory, Livermore, USA

J. Gronberg, D. Lange, F. Rebassoo, D. Wright

University of Maryland, College Park, USA

A. Baden, B. Calvert, S. C. Eno, J. A. Gomez, N. J. Hadley, R. G. Kellogg, T. Kolberg, Y. Lu, M. Marionneau, A. C. Mignerey, K. Pedro, A. Skuja, J. Temple, M. B. Tonjes, S. C. Tonwar

Massachusetts Institute of Technology, Cambridge, USA

A. Apyan, R. Barbieri, G. Bauer, W. Busza, I. A. Cali, M. Chan, L. Di Matteo, V. Dutta, G. Gomez Ceballos, M. Goncharov, D. Gulhan, M. Klute, Y. S. Lai, Y.-J. Lee, A. Levin, P. D. Luckey, T. Ma, C. Paus, D. Ralph, C. Roland, G. Roland, G. S. F. Stephans, F. Stöckli, K. Sumorok, D. Velicanu, J. Veverka, B. Wyslouch, M. Yang, A. S. Yoon, M. Zanetti, V. Zhukova

University of Minnesota, Minneapolis, USA

B. Dahmes, A. De Benedetti, A. Gude, S. C. Kao, K. Klapoetke, Y. Kubota, J. Mans, N. Pastika, R. Rusack, A. Singovsky, N. Tamba, J. Turkewitz

University of Mississippi, Oxford, USA

J. G. Acosta, L. M. Cremaldi, R. Kroeger, S. Oliveros, L. Perera, R. Rahmat, D. A. Sanders, D. Summers

University of Nebraska-Lincoln, Lincoln, USA

E. Avdeeva, K. Bloom, S. Bose, D. R. Claes, A. Dominguez, R. Gonzalez Suarez, J. Keller, D. Knowlton, I. Kravchenko, J. Lazo-Flores, S. Malik, F. Meier, G. R. Snow

State University of New York at Buffalo, Buffalo, USA

J. Dolen, A. Godshalk, I. Iashvili, S. Jain, A. Kharchilava, A. Kumar, S. Rappoccio

Northeastern University, Boston, USA

G. Alverson, E. Barberis, D. Baumgartel, M. Chasco, J. Haley, A. Massironi, D. Nash, T. Orimoto, D. Trocino, D. Wood, J. Zhang

Northwestern University, Evanston, USA

A. Anastassov, K. A. Hahn, A. Kubik, L. Lusito, N. Mucia, N. Odell, B. Pollack, A. Pozdnyakov, M. Schmitt, S. Stoynev, K. Sung, M. Velasco, S. Won

University of Notre Dame, Notre Dame, USA

D. Berry, A. Brinkerhoff, K. M. Chan, A. Drozdetskiy, M. Hildreth, C. Jessop, D. J. Karmgard, N. Kellams, J. Kolb, K. Lannon, W. Luo, S. Lynch, N. Marinelli, D. M. Morse, T. Pearson, M. Planer, R. Ruchti, J. Slaunwhite, N. Valls, M. Wayne, M. Wolf, A. Woodard

The Ohio State University, Columbus, USA

L. Antonelli, B. Bylsma, L. S. Durkin, S. Flowers, C. Hill, R. Hughes, K. Kotov, T. Y. Ling, D. Puigh, M. Rodenburg, G. Smith, C. Vuosalo, B. L. Winer, H. Wolfe, H. W. Wulsin

Princeton University, Princeton, USA

E. Berry, P. Elmer, V. Halyo, P. Hebda, J. Hegeman, A. Hunt, P. Jindal, S. A. Koay, P. Lujan, D. Marlow, T. Medvedeva, M. Mooney, J. Olsen, P. Piroué, X. Quan, A. Raval, H. Saka, D. Stickland, C. Tully, J. S. Werner, S. C. Zenz, A. Zuranski

University of Puerto Rico, Mayaguez, USA

E. Brownson, A. Lopez, H. Mendez, J. E. Ramirez Vargas

Purdue University, West Lafayette, USA

E. Alagoz, D. Benedetti, G. Bolla, D. Bortoletto, M. De Mattia, A. Everett, Z. Hu, M. K. Jha, M. Jones, K. Jung, M. Kress, N. Leonardo, D. Lopes Pegna, V. Maroussov, P. Merkel, D. H. Miller, N. Neumeister, B. C. Radburn-Smith, I. Shipsey, D. Silvers, A. Svyatkovskiy, F. Wang, W. Xie, L. Xu, H. D. Yoo, J. Zablocki, Y. Zheng

Purdue University Calumet, Hammond, USA

N. Parashar

Rice University, Houston, USA

A. Adair, B. Akgun, K. M. Ecklund, F. J. M. Geurts, W. Li, B. Michlin, B. P. Padley, R. Redjimi, J. Roberts, J. Zabel

University of Rochester, Rochester, USA

B. Betchart, A. Bodek, R. Covarelli, P. de Barbaro, R. Demina, Y. Eshaq, T. Ferbel, A. Garcia-Bellido, P. Goldenzweig, J. Han, A. Harel, D. C. Miner, G. Petrillo, D. Vishnevskiy, M. Zielinski

The Rockefeller University, New York, USA

A. Bhatti, R. Ciesielski, L. Demortier, K. Goulios, G. Lungu, S. Malik, C. Mesropian

Rutgers, The State University of New Jersey, Piscataway, USA

S. Arora, A. Barker, J. P. Chou, C. Contreras-Campana, E. Contreras-Campana, D. Duggan, D. Ferencek, Y. Gershtein, R. Gray, E. Halkiadakis, D. Hidas, A. Lath, S. Panwalkar, M. Park, R. Patel, V. Rekovic, J. Robles, S. Salur, S. Schnetzer, C. Seitz, S. Somalwar, R. Stone, S. Thomas, P. Thomassen, M. Walker

University of Tennessee, Knoxville, USA

K. Rose, S. Spanier, Z. C. Yang, A. York

Texas A&M University, College Station, USA

O. Bouhali⁶⁰, R. Eusebi, W. Flanagan, J. Gilmore, T. Kamon⁶¹, V. Khotilovich, V. Krutelyov, R. Montalvo, I. Osipenkov, Y. Pakhotin, A. Perloff, J. Roe, A. Safonov, T. Sakuma, I. Suarez, A. Tatarinov, D. Toback

Texas Tech University, Lubbock, USA

N. Akchurin, C. Cowden, J. Damgov, C. Dragoiu, P. R. Duderu, J. Faulkner, K. Kovitangoon, S. Kunori, S. W. Lee, T. Libeiro, I. Volobouev

Vanderbilt University, Nashville, USA

E. Appelt, A. G. Delannoy, S. Greene, A. Gurrola, W. Johns, C. Maguire, Y. Mao, A. Melo, M. Sharma, P. Sheldon, B. Snook, S. Tuo, J. Velkovska

University of Virginia, Charlottesville, USA

M. W. Arenton, S. Boutle, B. Cox, B. Francis, J. Goodell, R. Hirosky, A. Ledovskoy, C. Lin, C. Neu, J. Wood

Wayne State University, Detroit, USA

S. Gollapinni, R. Harr, P. E. Karchin, C. Kottachchi Kankanamge Don, P. Lamichhane

University of Wisconsin, Madison, USA

D. A. Belknap, L. Borrello, D. Carlsmith, M. Cepeda, S. Dasu, S. Duric, E. Friis, M. Grothe, R. Hall-Wilton, M. Herndon, A. Hervé, P. Klabbers, J. Klukas, A. Lanaro, A. Levine, R. Loveless, A. Mohapatra, I. Ojalvo, T. Perry, G. A. Pierro, G. Polese, I. Ross, A. Sakharov, T. Sarangi, A. Savin, W. H. Smith

† Deceased

- 1: Also at Vienna University of Technology, Vienna, Austria
- 2: Also at CERN, European Organization for Nuclear Research, Geneva, Switzerland
- 3: Also at Institut Pluridisciplinaire Hubert Curien, Université de Strasbourg, Université de Haute Alsace Mulhouse, CNRS/IN2P3, Strasbourg, France
- 4: Also at National Institute of Chemical Physics and Biophysics, Tallinn, Estonia
- 5: Also at Skobeltsyn Institute of Nuclear Physics, Lomonosov Moscow State University, Moscow, Russia
- 6: Also at Universidade Estadual de Campinas, Campinas, Brazil
- 7: Also at California Institute of Technology, Pasadena, USA
- 8: Also at Laboratoire Leprince-Ringuet, Ecole Polytechnique, IN2P3-CNRS, Palaiseau, France
- 9: Also at Zewail City of Science and Technology, Zewail, Egypt
- 10: Also at Suez University, Suez, Egypt
- 11: Also at British University in Egypt, Cairo, Egypt
- 12: Also at Cairo University, Cairo, Egypt
- 13: Also at Fayoum University, El-Fayoum, Egypt
- 14: Now at Ain Shams University, Cairo, Egypt
- 15: Also at Université de Haute Alsace, Mulhouse, France
- 16: Also at Joint Institute for Nuclear Research, Dubna, Russia
- 17: Also at Brandenburg University of Technology, Cottbus, Germany

- 18: Also at The University of Kansas, Lawrence, USA
 19: Also at Institute of Nuclear Research ATOMKI, Debrecen, Hungary
 20: Also at Eötvös Loránd University, Budapest, Hungary
 21: Also at Tata Institute of Fundamental Research-HECR, Mumbai, India
 22: Now at King Abdulaziz University, Jeddah, Saudi Arabia
 23: Also at University of Visva-Bharati, Santiniketan, India
 24: Also at University of Ruhuna, Matara, Sri Lanka
 25: Also at Isfahan University of Technology, Isfahan, Iran
 26: Also at Sharif University of Technology, Tehran, Iran
 27: Also at Plasma Physics Research Center, Science and Research Branch, Islamic Azad University, Tehran, Iran
 28: Also at Università degli Studi di Siena, Siena, Italy
 29: Also at Centre National de la Recherche Scientifique (CNRS)-IN2P3, Paris, France
 30: Also at Purdue University, West Lafayette, USA
 31: Also at Universidad Michoacana de San Nicolas de Hidalgo, Morelia, Mexico
 32: Also at National Centre for Nuclear Research, Swierk, Poland
 33: Also at Institute for Nuclear Research, Moscow, Russia
 34: Also at St. Petersburg State Polytechnical University, St. Petersburg, Russia
 35: Also at Faculty of Physics, University of Belgrade, Belgrade, Serbia
 36: Also at Facoltà Ingegneria, Università di Roma, Rome, Italy
 37: Also at Scuola Normale e Sezione dell'INFN, Pisa, Italy
 38: Also at University of Athens, Athens, Greece
 39: Also at Paul Scherrer Institut, Villigen, Switzerland
 40: Also at Institute for Theoretical and Experimental Physics, Moscow, Russia
 41: Also at Albert Einstein Center for Fundamental Physics, Bern, Switzerland
 42: Also at Gaziosmanpasa University, Tokat, Turkey
 43: Also at Adiyaman University, Adiyaman, Turkey
 44: Also at Cag University, Mersin, Turkey
 45: Also at Mersin University, Mersin, Turkey
 46: Also at Izmir Institute of Technology, Izmir, Turkey
 47: Also at Ozyegin University, Istanbul, Turkey
 48: Also at Kafkas University, Kars, Turkey
 49: Also at Istanbul University, Faculty of Science, Istanbul, Turkey
 50: Also at Mimar Sinan University, Istanbul, Istanbul, Turkey
 51: Also at Kahramanmaraş Sütcü Imam University, Kahramanmaraş, Turkey
 52: Also at Rutherford Appleton Laboratory, Didcot, UK
 53: Also at School of Physics and Astronomy, University of Southampton, Southampton, UK
 54: Also at INFN Sezione di Perugia; Università di Perugia, Perugia, Italy
 55: Also at Utah Valley University, Orem, USA
 56: Also at University of Belgrade, Faculty of Physics and Vinca Institute of Nuclear Sciences, Belgrade, Serbia
 57: Also at Argonne National Laboratory, Argonne, USA
 58: Also at Erzincan University, Erzincan, Turkey
 59: Also at Yildiz Technical University, Istanbul, Turkey
 60: Also at Texas A&M University at Qatar, Doha, Qatar
 61: Also at Kyungpook National University, Taegu, Korea

The TOTEM Collaboration

G. Antchev¹⁵, P. Aspell⁸, I. Atanassov^{8,a}, V. Avati⁸, J. Baechler⁸, V. Berardi^{5a,5b}, M. Berretti^{7b}, E. Bossini^{7b}, U. Bottigli^{7b}, M. Bozzo^{6a,6b}, E. Brücken^{3a,3b}, A. Buzzo^{6b}, F. S. Cafagna^{5a}, M. G. Catanesi^{5a}, C. Covault⁹, M. Csanád^{4,d}, T. Csörgő⁴, M. Deile⁸, M. Doubek^{1b}, K. Eggert⁹, V. Eremin¹², A. Fiergolski^{5a,b}, F. Garcia^{3a}, V. Georgiev¹¹, S. Giani⁸, L. Grzanka^{10,c}, J. Hammerbauer¹¹, J. Heino^{3a}, T. Hilden^{3a,3b}, A. Karev⁸, J. Kašpar^{1a,8}, J. Kopal^{1a,8}, J. Kosinski¹⁰, V. Kundrát^{1a}, S. Lami^{7a}, G. Latino^{7b}, R. Lauhakangas^{3a}, T. Leszko¹⁶, E. Lippmaa², J. Lippmaa², M. V. Lokajčiček^{1a}, L. Losurdo^{7b}, F. Lucas Rodríguez⁸,

M. Macri^{6b}, T. Mäki^{3a}, A. Mercadante^{5a}, N. Minafra^{5b,8}, S. Minutoli^{6b}, F. Nemes^{4,d}, H. Niewiadomski⁸, E. Oliveri^{7b}, F. Oljemark^{3a,3b}, R. Orava^{3a,3b}, M. Oriunno¹³, K. Österberg^{3a,3b}, P. Palazzi^{7b}, Z. Petroutka¹¹, J. Procházka^{1a}, M. Quinto^{5a,5b}, E. Radermacher⁸, E. Radicioni^{5a}, F. Ravotti⁸, L. Ropelewski⁸, G. Ruggiero⁸, H. Saarikko^{3a,3b}, A. Scribano^{7b}, J. Smajek⁸, W. Snoeys⁸, J. Sziklai⁴, C. Taylor⁹, N. Turini^{7b}, V. Vacek^{1b}, J. Weltri^{3a,3b}, J. Whitmore¹⁴, P. Wyszowski¹⁰, K. Zielinski¹⁰

^{1 a} Institute of Physics of the Academy of Sciences of the Czech Republic, Praha, Czech Republic

^{1 b} Czech Technical University, Praha, Czech Republic

² National Institute of Chemical Physics and Biophysics NICPB, Tallinn, Estonia

^{3 a} Helsinki Institute of Physics, Helsinki, Finland

^{3 b} Department of Physics, University of Helsinki, Helsinki, Finland

⁴ MTA Wigner Research Center, RMKI, Budapest, Hungary

^{5 a} INFN Sezione di Bari, Bari, Italy

^{5 b} Dipartimento Interateneo di Fisica di Bari, Bari, Italy

^{6 a} Università degli Studi di Genova, Genova, Italy

^{6 b} Sezione INFN di Genova, Genova, Italy

^{7 a} INFN Sezione di Pisa, Pisa, Italy

^{7 b} Università degli Studi di Siena and Gruppo Collegato INFN di Siena, Siena, Italy

⁸ CERN, Geneva, Switzerland

⁹ Case Western Reserve University, Department of Physics, Cleveland, OH, USA

¹⁰ AGH University of Science and Technology, Krakow, Poland

¹¹ University of West Bohemia, Pilsen, Czech Republic

¹² Ioffe Physical - Technical Institute of Russian Academy of Sciences, St. Petersburg, Russia

¹³ SLAC National Accelerator Laboratory, Stanford, CA, USA

¹⁴ Penn State University, Department of Physics, University Park, PA, USA

¹⁵ INRNE-BAS, Institute for Nuclear Research and Nuclear Energy, Bulgarian Academy of Sciences, Sofia, Bulgaria

¹⁶ Warsaw University of Technology, Warsaw, Poland

^a Also at INRNE-BAS, Institute for Nuclear Research and Nuclear Energy, Bulgarian Academy of Sciences, Sofia, Bulgaria

^b Also at Warsaw University of Technology, Warsaw, Poland

^c Also at Institute of Nuclear Physics, Polish Academy of Science, Cracow, Poland

^d Also at Department of Atomic Physics, Eötvös University, Budapest, Hungary